

**APPLICATIONS OF RECEPTOR MODELING METHODS  
TO SOURCE APPORTIONMENT OF ARSENIC IN  
THE RUSTON-TACOMA, WASHINGTON AIRSHED:  
A FEASIBILITY STUDY**

**FINAL REPORT**

**Prepared For:  
Puget Sound Air Pollution Control Agency  
200 W. Mercer Street, Room 205  
Seattle, Washington 98109**

**By:  
NEA, INC.  
10950 S.W. 5th Street, Suite 380  
Beaverton, Oregon 97005**

**June 15, 1984**

APPLICATIONS OF RECEPTOR MODELING METHODS  
TO SOURCE APPORTIONMENT OF ARSENIC IN  
THE RUSTON-TACOMA, WASHINGTON AIRSHED:  
A FEASIBILITY STUDY

Final Report

Prepared For:

Puget Sound Air Pollution Control Agency  
200 W. Mercer Street, Room 205  
Seattle, Washington 98109

By

John A. Cooper  
James E. Houck  
Lyle C. Pritchett  
and  
Clifton A. Frazier

NEA, INC.  
10950 S.W. 5th Street, Suite 380  
Beaverton, Oregon 97005

June 15, 1984

## ABSTRACT

The feasibility of using receptor modeling methods to apportion sources of arsenic in the Tacoma-Ruston airshed near the ASARCO, Incorporated copper smelter has been evaluated. Source resolvability and quantification was evaluated by chemically characterizing representative fine and coarse particle sources within the smelter and settled dust samples outside the smelter. The elemental composition of ten ambient particulate samples was also measured and arsenic levels apportioned using chemical mass balance methods.

It was concluded that receptor modeling using only chemical information would probably not be able to adequately resolve and quantify the influence of all key sources. It was also concluded, however, that one could confidently expect to resolve all major sources responsible for high arsenic levels by separating the ambient aerosol into fine and coarse particles interpreting the data with both chemical mass balance and multivariate analysis methods and relating these results to meteorologically regime stratified arsenic data.

Upper limits for the contributions of several sources were established as a result of the ambient filter analysis. It was also concluded from the ambient filter analysis that coarse particle sources are probably responsible for the majority of arsenic on high impact days studied.

## ACKNOWLEDGEMENTS

Completion of this study is the result of the support and cooperation of a number of organizations and individuals. Support for this study was provided by the Puget Sound Air Pollution Control Agency (PSAPCA) through a grant from the Region X Environmental Protection Agency. Washington State Department of Ecology (WSDOE) provided staff assistance with source sampling and ASARCO, Inc. provided both plant access and staff assistance with source sampling.

The source sampling assistance of Jim Nolan of PSAPCA and Jay Willenberg of WSDOE is also gratefully acknowledged, as well as the many helpful suggestions from Jim Nolan, who was also PSAPCA's program director. The cooperation and assistance of the ASARCO staff, both in Tacoma and Salt Lake City was particularly helpful and is gratefully acknowledged.

## TABLE OF CONTENTS

	<u>Page</u>
ABSTRACT	i
ACKNOWLEDGEMENTS	ii
LIST OF TABLES	iv
LIST OF FIGURES	v
1.0 INTRODUCTION	1
2.0 OBJECTIVES AND CRITERIA	2
3.0 EXPERIMENTAL	4
3.1 Source Sampling	4
3.2 Ambient Aerosol Samples	6
3.3 Elemental Analysis	6
4.0 RESULTS AND DISCUSSION	7
4.1 Fine to Coarse Particle Size Ratios	7
4.2 Elemental Analysis Results for Source Samples	8
4.3 Elemental Analysis Results for Ambient Samples	10
4.4 Chemical Mass Balance (CMB) Results	11
4.5 Source Resolution	12
4.6 Indirect Contribution of Historical Contamination	13
5.0 CONCLUSIONS	15
6.0 RECOMMENDATIONS	15
7.0 REFERENCES	18

# LIST OF TABLES

<u>Number</u>	<u>Title</u>	<u>Page</u>
1	List of Potential Arsenic Sources and Estimated Emission Rates (kg/hr) <sup>11</sup>	21
2	Summary of Sampling Data for Process Emissions Sampled at the ASARCO - Tacoma Copper Smelter	22
3	Summary of Resuspension Data for Bulk Source Samples Collected from the ASARCO - Tacoma Copper Smelter	23
4	Average Fine to Coarse Particle Ratios After Correcting for Fine Particles Deposited on Coarse Particle Filter	24
5	Percent Elemental Composition of Herreschoff Roaster Charge and Calcine	25
6	Percent Elemental Composition of Particles in Road and Railroad Track Dust	26
7	Percent Elemental Composition of Slag	27
8	Percent Elemental Composition of High Arsenic Bulk Samples	28
9	Percent Elemental Composition of Settled Dust Collected Within the Plant and the Ore Concentrate	29
10	Percent Elemental Composition of Emission from Number 1 Brick Flue: Fine Fraction ( < 2.5 $\mu\text{m}$ )	30
11	Percent Elemental Composition of Emission from Number 4 Converter Secondary Hood: Fine Fraction ( < 2.5 $\mu\text{m}$ )	31
12	Percent Elemental Composition of Emission from Reverbatary Furnace Slag Skim: Fine Fraction ( < 2.5 $\mu\text{m}$ )	32
13	Percent Elemental Composition of Emissions from Number 1 Brick Flue: Coarse Fraction ( > 2.5 $\mu\text{m}$ ) <sup>a</sup>	33
14	Percent Elemental Composition of Emissions from the Number 4 Converter Secondary Hood: Coarse Fraction ( > 2.5 $\mu\text{m}$ ) <sup>a</sup>	34
15	Percent Elemental Composition of Emissions from Reverbatary Furnace Slag Skim: Coarse Fraction ( > 2.5 $\mu\text{m}$ )	35
16	Comparison of Elemental Composition of Slag	36
17	Elemental Concentration of Ambient Samples ( $\mu\text{g}/\text{m}^3$ )*	37
18a	Correlation Matrix (10 Ambient glass fiber filters)	38
18b	Slope Matrix (10 Ambient glass fiber filters)	38
18c	Intercept Matrix (10 Ambient glass fiber filters)	38

# LIST OF TABLES (Continued)

<u>Number</u>	<u>Title</u>	<u>Page</u>
19	CMBDEQ Results for CMB #MB338	39
20	CMBDEQ Results for CMB #MB338	39
21	CMBDEQ Results for CMB #MB338	40
22	CMBDEQ Results for CMB #MB338	41
23	CMBDEQ Results for CMB #MB335	41
24	CMBDEQ Results for CMB #MB335	42
25	CMBDEQ Results for CMB #MB336	42
26	CMBDEQ Results for CMB #MB337	43
27	CMBDEQ Results for CMB #MB337	43
28	CMBDEQ Results for CMB #MB334	44
29	CMBDEQ Results for CMB #MB334	44
30	CMBDEQ Results for CMB #MB033	45
31	CMBDEQ Results for CMB #MB033	45
32	CMBDEQ Results for CMB #MB037	46
33	CMBDEQ Results for CMB #MB037	46
34	CMBDEQ Results for CMB #MB029	47
35	CMBDEQ Results for CMB #MB032	47
36	CMBDEQ Results for CMB #MB038	48
37	List of Source Code Definitions	49
38	Maximum Source Contributions	50

## LIST OF FIGURES

<u>Number</u>	<u>Title</u>	<u>Page</u>
1	Plot of the percent Al and Si for combustion and geological sources. These sources would be difficult to resolve using only these two elements (dimensions).	51
2	Three dimensional plot of the Fe, Al, and Si in geological type samples. The addition of the Fe dimension effectively improved the source resolving capability, i.e., the angle between the coal fly ash and crustal average has increased.	52
3	Three dimensional plot for the As, Al, and Si composition in geological samples. The addition of As has greatly improved the separation of the fine coal fly ash from the other sources. Other coal fly ash samples have been reported to contain even higher As concentrations.	52
4	Physical layout of the ASARCO-Tacoma smelter showing the location of the bulk samples collected for analysis.	53
5	Vectorial representation of three elements from selected source profiles.	54
6	Vectorial representation of three elements from selected source profiles.	55
7	Schematic categorization of sources based on chemistry and particle size	56
8	Illustration of direct and indirect smelter impacts on air quality. (From Kellogg, report, NEA).	57
9	Schematic diagram of the sources and sinks of aerosolizable dust.	57
10	Percent quarterly lead levels at Silver King School Kellogg, Idaho.	58
11	Percent quarterly lead levels at a doctor's clinic in Kellogg, Idaho.	59



## 1.0 INTRODUCTION

ASARCO, Incorporated (ASARCO) currently operates a primary copper smelter in the Tacoma-Ruston, Washington area. The smelter began operation in 1890 as a lead smelter, and was later converted to a copper smelter capable of processing high arsenic copper ores. Operation of the smelter over the past century has contaminated the local area with hazardous elements such as arsenic, cadmium and lead, as well as other elements. Although emission rates of these elements have been reduced substantially in recent years by the addition of pollution control equipment, arsenic levels are still high and of concern.

Section 112 (b) (1) (B) of the Clean Air Act (42 U.S.C. 7412) requires establishment of national emission standards for hazardous air pollutants (NESHAP) which will effectively maintain ambient air quality. To do this, however, requires the development of control strategies based on an accurate, quantitative knowledge of the major sources within a plant responsible for high levels of hazardous pollutants such as arsenic.

Numerous emission inventory and dispersion modeling studies of the smelter have been conducted in recent years. (1-11) The results from these studies, however, have not provided an adequate level of understanding to develop and implement a control strategy with a high level of confidence that it will be effective in improving air quality. These classical dispersion modeling methods are severely limited in this particular case because of the complex terrain, unknown micrometeorology, and difficulty of modeling low level fugitive emissions which exhibit large variations in daily absolute emission rates, in addition to there being potentially large contributions from frequent accidental releases.

Receptor modeling methods, (12-14) however, require only a knowledge of the relative chemical and physical characteristics of

emissions to quantitatively apportion source contributions to particulate levels. This approach, in contrast to dispersion modeling, does not require absolute emission rates or meteorological data. These methods have been successfully applied to numerous other complex airsheds, including four airsheds with lead smelters. Quantitative source impacts are calculated with receptor methods based on the relative chemical composition of an ambient aerosol at a receptor and that of potential source emissions. A major limitation of this method is that it cannot resolve the influence of sources having similar chemical composition unless other features, such as particle size, time and spatial variability, etc. are included in the analysis.

This problem of potentially poor source resolution due to similar chemistry (multicollinearity) is of particular concern with respect to the Tacoma-Ruston smelter, because many of its sources of arsenic are expected to have a similar chemical composition.

The objective of this study is to evaluate the feasibility of using receptor modeling methods to identify and quantify the contribution major arsenic sources within the ASARCO smelter make to ambient arsenic concentrations.

The approach taken is to first define potential study objectives to be met or hypotheses tested by a receptor model study, establish evaluation criteria, and characterize potential major arsenic sources to determine if they are potentially resolvable.

## 2.0 OBJECTIVES AND CRITERIA

The feasibility and success of any study depends on how complete its objectives are met and hypotheses answered. Although it is clear that the objective of any receptor modeling study would be to identify and quantify major arsenic sources within the smelter, it is just as clear that this objective can only be met to a degree within practical limits of resources. It is thus essential to establish

source impact hypotheses based on previous studies, and then ask which of these specific sources can be resolved and quantified.

Potential arsenic sources have been divided by the EPA (11) into process and fugitive emissions as indicated in Table 1. Indirect resuspension has been added to account for the potential contribution contaminated road and soil dust make to ambient levels. The question now is whether or not the converters fugitive emissions can be resolved from the process ducted emissions, slag and matte tapping, miscellaneous or arsenic building emissions.

The criteria for receptor modeling feasibility are thus based on (1) the ability of a receptor modeling study to resolve the impacts of the potential major sources, and (2) quantify the impacts of the major sources.

Source resolution is discussed in detail in reference 16. It refers primarily to the degree of difference in the characteristic features associated with each source. These features can include

- chemical composition
- particle size
- point of emission (height, geographical), and
- time variability patterns.

Source resolution from the chemical point-of-view, refers to the angle between two source vectors when plotted in elemental space. Examples of this are illustrated in Figures 1-3. Figure 1 is a plot of the Al and Si concentration of soil, road dust, coal, fly ash, average earths crust, asphalt production, and emissions from a rock crusher. The coordinates of each data point represents the end point of a vector from the origin to the data point. The influence of these sources could not be easily resolved on the basis of their Al and Si chemistry alone. That is the angle between the vectors leading to each data point is small relative to the uncertainties. The angle between source vectors can be increased, however, by increasing the dimensionality of the space as illustrated in Figure 2,

which shows the addition of Fe. In this case, the solid angle between the sources has been increased, but only slightly. The addition of an As dimension greatly improves the resolvability of fine particle coal fly ash from the other crustal sources. Further source resolvability could be obtained by collecting only fine particles, since 90 to 95% of soil derived material is greater than 2.5  $\mu\text{m}$ , and road dust can be further resolved from soil because of their characteristic traffic and windspeed dependencies.

Although a source may be easily resolved, it may not be accurately quantified because of a highly variable chemical composition. The mass attributed to a particular source is directly proportional to the chemical composition of the fitting elements used in the source profile. Large uncertainties in these source profiles yield large uncertainties in source contributions, even though it may be readily resolvable from other interfering sources.

### 3.0 EXPERIMENTAL

#### 3.1 Source Sampling

Samples of emissions from selected potential sources were collected and analyzed to determine which key sources could be resolved, based on their chemical composition and particle size characteristics. Source samples collected are listed in Tables 2 and 3. Although the sources sampled do not include all potential sources, they represent those sources thought to be major contributors and are representative of the range of emissions expected.

NEA's size-segregating dilution sampler (SSDS) (17) was used to collect fine and coarse particle samples of the emissions in the number 1 brick flue which are representative of the stack emissions. This sampler extracts an isokinetic sample, dilutes and cools the emissions to near ambient conditions, and separates the particles into fine ( $< 2.5 \mu\text{m}$  and coarse ( $> 2.5 \mu\text{m}$ ) particle fractions with a virtual dichotomous impactor.

The lower temperature emissions from slag tapping and the secondary converter hood were sampled both with a virtual dichotomous impactor and a low-volume TSP sampler. Although the converter emissions were sampled in the secondary hood, they are expected to be representative of fugitive emissions from converters in general. The slag tapping emissions sampled are expected to be representative of emissions during slag dumping.

Bulk samples of fifteen representative fugitive dust sources were collected by PSAPCA staff. Road dust samples were collected with NEA's paved road dust sampler, which collects the material on a glass fiber filter. The locations where the bulk samples were collected are indicated on the map shown in Figure 4.

Samples collected with NEA's SSDS, dichotomous sampler, and the low-volume TSP sampler were returned to the laboratory where the filters were weighed and analyzed nondestructively by X-ray fluorescence without prior sample preparation.

Four high arsenic bulk samples were resuspended without further preparation, while the other bulk samples were dried at 65°C overnight and sieved prior to resuspension.

Material passing through a 400 mesh screen (38  $\mu\text{m}$ ) was aerosolized in NEA's resuspension chamber and sampled with a virtual impactor dichotomous sampler. Fine ( < 2.5  $\mu\text{m}$ ) and coarse ( > 2.5  $\mu\text{m}$ , < 15  $\mu\text{m}$ ) particle samples were collected on teflon filters and weighed. The aerosolization process was continued until an appropriate amount of mass was deposited on each filter. Because of the predominance of coarse particles in the bulk samples, the coarse particle filters reached appropriate deposit levels much more rapidly than the fine particle filter. The fine to coarse (F/C) particle ratio was determined from the filter deposit masses measured when the appropriate mass level was reached on the coarse particle filter. The coarse particle filter was then replaced with a scrap teflon filter, and the aerosolization-sample collection process continued until a sufficient level of material was collected on the fine filter for analysis.

The aerosolization chamber and dichotomous sampler were both completely dismantled and thoroughly cleaned between each sample to minimize the possibility of contamination. Samples containing the lowest arsenic and lead concentrations were aerosolized prior to those with high arsenic concentration to further minimize the possibility of contamination.

The slag dump fines and Lepanto copper ore concentrates were aerosolized and sampled with a low-volume TSP sampler, because none of the material passed through the 400 mesh (38  $\mu$ m) screen.

### 3.2 Ambient Aerosol Samples

Ten ambient aerosol samples were selected by PSAPCA for analysis to represent high arsenic impact days. The samples were collected with high-volume TSP samplers on glass fiber filters at sampling sites P2 (26th & Pearl), P14 (47th and Baltimore), and P15 (Rustin Elementary School). The P2 site is located about two miles southeast of the plant. The P14 site is two blocks east of the main stack, and the P15 site is across the street from the plant parking lot, south of the smelter. Disks 47 mm in diameter were cut from the filters for X-ray fluorescence analysis.

### 3.3 Elemental Analysis

The elemental composition of source and ambient aerosol samples was determined using energy-dispersive X-ray fluorescence analysis. Standard thin-film methods (18, 19) were used to quantify the elemental composition of the deposits.

Special analysis conditions, however, were required because of the unusual elemental ratios. Analyte lines (K-X-rays) for Ag, Cd, In and Sn have spectral interferences from the As and Pb sum peaks. These interferences were eliminated by analyzing the samples using post copper filters to absorb the As and Pb X-rays prior to analysis. L - X-ray lines from As, Ag, Cd, In, Sn, and Sb also interfered

with the analysis of light elements, such as Mg, Al, K, and Ca, which substantially increased the minimum detection limits for these elements.

The glass-fiber filter analysis was limited by its high elemental blank content, and, as a result, only a few elements could be reliably quantified on these filters.

Some elements, such as Tl and Bi, were observed, but only semi-quantitative results were reported because validated standards were not available.

#### 4.0 RESULTS AND DISCUSSION

##### 4.1 Fine to Coarse Particle Size Ratios

The fine to coarse particle size ratios were determined using virtual dichotomous impactors with fine to coarse size cuts as follows:

Process Samples

Fine: < 2.5  $\mu\text{m}$

Coarse: > 2.5  $\mu\text{m}$

Bulk Aerosolized Samples

Fine: < 2.5  $\mu\text{m}$

Coarse: > 2.5  $\mu\text{m}$  but < 15  $\mu\text{m}$

The main difference between the process samples and the bulk samples was in the upper cut point for the coarse particle fraction. An upper cut point for the coarse particles in the process emissions was not established, while the standard 15  $\mu\text{m}$  inlet was used to sample the aerosolized bulk samples. This will have essentially no impact on the characteristics of material collected with similar samplers with 15  $\mu\text{m}$  cut points in the ambient environment because the fraction of coarse particles in the process emissions is so small.

The F/C particle ratios for the aerosolizable bulk samples were based on intermediate mass determinations made after enough material had been collected on the coarse particle filter. The fine particle mass listed is the mass obtained after additional aerosolization steps

using a scrap coarse particle filter. The listed fine particle mass was not used in the F/C particle ratio calculations.

The average F/C particle ratios are listed in Table 4. The sources are easily grouped into fine particle process emission sources in which about 95% of the particulate mass is less than 2.5  $\mu\text{m}$ , and coarse particle bulk samples representing fugitive dust sources in which coarse particles represent more than 90% of the mass.

The fine to coarse particle ratio for the "Slag Dump Fine" sample and the Lepanto Copper Ore Concentrate could not be determined because insufficient material passed through the 400 mesh sieve ( $< 38 \mu\text{m}$ ).

This clear distinction between fine and coarse particles will be particularly valuable in resolving the influence of possible sources.

#### 4.2 Elemental Analysis Results for Source Samples

Elemental analysis results are presented for the source samples in Tables 5-15. The elemental composition obtained in this study for the coarse particle fraction of the composite slag sample (Table 7) is compared in Table 16 with an earlier bulk analysis of slag using semiquantitative spectrographic analysis and atomic absorption methods. (7) Good agreement is obtained for most elements, particularly when one considers that the analysis results are based on completely different slag samples. The main exceptions are iron, which differs by a factor of two, and copper and lead which differ by 20 to 4 fold. Still lower iron concentrations were measured in the fine particle fraction of the slag samples analyzed in this study (Table 7). This difference in a major species, such as iron, is thought to be due to differences in samples and not an analytical artifact associated with this analysis.

Errors greater than indicated in the tables can exist for the coarse filters collected from the aerosolized bulk samples because of



the loss of particles prior to analysis. The coarse particles were poorly held to the teflon filters, and great care in handling was required to minimize particle loss after weighing. Even so, some coarse particles were lost from the filters as determined by weighing the filter after XRF analysis. In cases where particle loss was indicated, the weights after XRF analysis were used to calculate the percent composition. This potential problem, however, is not expected to affect the elemental ratios which are used in resolving the influence of specific sources. It would affect the quantification, but could be minimized in any future study by using oil coated filters which have been demonstrated to minimize the loss of particles even after being dropped in a shipping container. (20)

The sampling and analysis replication is best illustrated by the analysis results for the process samples. (Tables 10-15) The variability in the values obtained for the fine fraction samples representing slag dumping emissions and the stack emissions was in the 10 to 15% range over four samples collected over a period of sixteen hours for the slag samples, and 37 hours for the stack samples. The mass determinations for the process samples were quite stable and easily replicated. Thus, the uncertainties in the absolute percent compositions are expected to be accurately represented by the indicated uncertainties.

The uncertainties in the coarse particle composition of the process emissions is quite high because there was limited amount of mass collected on these filters to begin with, and the coarse particle composition was calculated by subtracting the fine particle mass that had deposited on the coarse particle filters. The resulting large uncertainties in the coarse particle fraction of the process emissions will not have a substantial impact on the feasibility of any receptor modeling study, because of the small contribution they are expected to make to ambient levels.

The bulk samples can be divided into two categories: samples

with high Al and Si, and those with low Al and Si concentrations. The four high As samples (SO<sub>2</sub> Cottrell dust, No. 1 flue dust, As baghouse pad dust and the As plant product), and the Lepanto copper ore concentrate fall into the latter category of low Al and Si content. Within this category, the ore concentrate is easily separated from the other fine sources based on its high Fe and Cu concentration relative to As, Pb and Sb. The SO<sub>2</sub> Cottrell dust is also characteristically different because of its high Pb concentration relative to Sb, As, Cu, An, and Fe. The No. 1 flue dust falls in between the Cottrell dust and the two remaining samples (As baghouse pad dust, and the As plant product) which are quite similar in composition.

The three process emissions fall into two easily distinguishable categories: one consisting of the slag dumping (skimming) emissions having high As concentrations relative to Pb, and the other category consisting of the converter and stack emissions having Pb levels comparable to the As concentrations.

These general categories are simply established on the basis of easily recognizable differences. Further categorization may be possible by taking into account more subtle differences in chemistry.

#### 4.3 Elemental Analysis Results for Ambient Samples

The elemental compositions of ten high arsenic ambient aerosol samples are listed in Table 17. The samples were collected on glass fiber filters with high-volume TSP samplers. The analysis of these samples was limited because of the high elemental background concentrations in the glass fiber filters, and their high degree of variability. The concentration of Fe, Cu, As, and Pb are about 1%, while the concentration of Sb runs about 0.1%. These concentrations are about 10 fold above the blank filter concentrations, and are not expected to be substantially affected by variations in blank concentrations.

Table 18 summarizes the results of bivariate plots of these five elements. From the correlation matrix in Table 18a it appears that Cu, As, Sb, and Pb are highly correlated, even after accounting for the correlation affect due to common variability caused by meteorology. Although it is difficult to draw strong conclusions from this very limited data set, it suggests that the variability of copper and lead, for example, is dominated by a single source or a group of interdependent sources with an average copper to lead ratio of about 1.55. There are a number of sources with Cu to Pb ratios close to this value, such as road dust, railroad track dust, slag, As baghouse pad dust, and the final product. On the other hand, a number of other sources, such as process emissions, could be eliminated as substantial contributors to these species because of their very low Cu to Pb ratios, unless these sources were highly dependent on another source with a very high Cu to Pb ratio. Other conclusions might be reached by examining other correlations and elemental ratios. With larger data sets, source profiles, and particle size information, potential sources can often be quickly eliminated or identified as a possible contributor with a high degree of confidence using multivariate analysis techniques such as factor analysis.

#### 4.4 Chemical Mass Balance (CMB) Results

The five elements, Fe, Cu, As, Sb, and Pb, with the highest degree of confidence from the analysis of the ambient filters were selected for inclusion in our CMB analysis. The CMB results from selected calculations are listed in Tables 19-36. The source codes are defined in Table 37. It is clear from these results that a number of possible source combinations could explain the limited ambient data.

Even though the most probable source contributions cannot be unambiguously defined on the basis of CMB analysis of the limited ambient data, definitive results concerning the maximum impact from some sources and the likely characteristics of other sources can be derived from even this limited ambient data set.

Table 38 lists the maximum possible impacts from a selected set of sources for 4 of the days with highest As levels. These maximum impacts were calculated by assuming all of the Fe or Cu was contributed by the source listed in the table. Since other sources are certain to have contributed to these relatively common elements, the actual contribution each source makes to As levels is expected to be much less.

In some cases, this maximum level is not too restrictive as indicated by the railroad track dust near the south gate and other high As sources not listed. On the other hand, it is clear that slag could not have contributed more than about 10% of the As and probably a lot less since much of the Fe is usually derived from road and other windblown dust.

The high Cu to As ratio in the ambient particles suggests the need for a substantial contribution from sources with high Cu concentrations. Since fine particle process emissions from the stack, converter, and slag pouring are deficient in Cu, coarse particle sources such as roaster calcines, etc., must have made substantial contributions to Cu levels, as well as As levels. Although high Cu sources cannot explain all or even most of the As, their contribution, which is required to explain Cu levels, suggests mechanisms which might cause other high As coarse particle sources to make substantial contributions to ambient As concentrations.

Additional source contribution restrictions, as well as more precisely defined CMB source contributions could be developed with fine and coarse particle sampling and measurement of more elements in the ambient aerosol.

#### 4.5 Source Resolution

Measurement of additional elements in the ambient aerosol would greatly improve the method's ability to resolve the influence of specific source impacts. The affect of adding different elements is

illustrated with the two plots shown in Figures 5 and 6. Figure 5 shows that three source groups can be resolved if their elemental concentrations are plotted in the As-Pb-Cu coordinate system shown. In this system, however, slag particles cannot be resolved from other sources such as the Martin Mill and Herreshoff roaster. Figure 6, however, shows the same sources but plotted in a coordinate system in which the Pb has been replaced by Fe. In this coordinate system, there are nearly three orthogonal source groups. The slag which was previously unresolved is now completely resolved from the other sources.

Figure 7 shows a schematic flow diagram in which sources are successively resolved based on the addition of elemental content information, particle size, or emission characteristics. Although not all of these sources would be resolved as simply as indicated, from a real ambient sample, it is likely that the influence of key contributing sources could be resolved with appropriate experimental design.

In addition, other chemical and physical features can be measured and used to resolve source influences. Of particular interest is the chemical form of As and S. Distinction between sulfide and sulfate and arsenic trioxide and pentoxide might be useful. This feasibility study did evaluate the utility of making compound distinctions, but a definitive conclusion on the utility of this type of data was not reached. Wet chemical, ion chromatographic and X-ray diffraction methods were considered (21-33), but not evaluated in the laboratory because (1) the species are not stable in the environment and their quantitative utility would have to be established prior to their use, (2) the cost of the analyses appeared to be high, and (3) preliminary indications suggested that additional speciation might not be necessary. In addition, private communications (34) and review of recent literature was not encouraging (21-38).

#### 4.6 Indirect Contribution of Historical Contamination

This smelter has been in operation in the Ruston area for nearly a century. During this time its emissions have contaminated the local

area with As and other hazardous elements. The indirect contribution of historical contamination has been thought to be a significant potential contributor of current ambient As levels.

Indirect area sources of As and other pollutants are defined as sources of aerosolizable dust which has been previously contaminated by the smelter. Figure 8 illustrates a comparative example of direct and indirect sources of pollutants, both of which originate from the smelter. Although there are many different types of surfaces which can act as indirect sources, there are only two significant resuspension forces, traffic and wind. Even though both of these resuspension forces yield emissions with similar chemical composition, their impacts can be easily resolved on the basis of significantly different time dependence.

The contaminated surfaces can have significantly different physical and chemical characteristics. A physical model describing the aerosolizable dust layer (39) on contaminated surfaces is illustrated in Figure 9. The aerosolizable dust layer by definition must be quite mobil and have a relatively short lifetime. The transition zone, on the other hand, could vary from zero on paved roads, roofs, etc. to a foot thick in tilled gardens. The bulk chemistry of the aerosolizable dust layer on unpaved dirt (soil) surfaces will take on the bulk soil composition plus the fallout impurities. The aerosolizable dust layer on leaves and roofs will consist primarily of the average fallout composition. The aerosolizable dust layer on paved roads will consist of a mixture of material from transportation sources (oil, brakes, exhaust, etc.), tracked-on soil, road wear and fallout. Paved road dust, however, is usually very similar in bulk chemical composition to the surrounding soils plus fallout impurities.

Of critical importance is the lifetime of pollutants in this aerosolizable dust layer. The lifetime of pollutants on paved surfaces must be short because of the forces acting on their removal

and the absence of a transition zone. This has been confirmed by measuring the rate ambient particulate lead concentrations decreased in Kellogg, Idaho, after closure of the Bunker Hill lead smelter in 1981. Figures 10 and 11 show that the time required for the ambient particulate levels to decrease to half their average value during the plant operation is about 4 months. It should also be noted that ambient levels are now averaging about  $0.2 \mu\text{g}/\text{m}^3$  which is the level calculated by CMB methods prior to plant closure for automotive tailpipe contributions. Thus, As in the aerosolizable dust layer on paved surfaces is likely to have originated from very recent fallout, mainly from the smelter, and track-out or erosion from contaminated soil.

## 5.0 CONCLUSIONS

- Receptor modeling based solely on particulate chemistry cannot resolve and quantify the contribution each potential source makes to ambient arsenic levels.
- Receptor modeling combined with fine and coarse particle sampling, multivariate analysis, and meteorological regime stratification of ambient levels can confidently be expected to resolve the influence of major sources and accurately quantify their contributions.
- Historical contamination of the area is not a significant cause of high ambient levels of As.
- Resuspension of recently contaminated road dust and other area dusts may be significant (about 5 to 10%) contributors to high As levels.
- Coarse particle sources are thought to be responsible for the majority of the ambient As, if the high As days studied are typical of high As days throughout the year.

## 6.0 RECOMMENDATIONS

A receptor modeling study of the Tacoma-Ruston ASARCO copper smelter is recommended on the basis of this feasibility study. This recommended study should include the following components to effectively

resolve and quantify the contribution major sources make to high As impact days:

1. Historical As and meteorological data should be used to develop a meteorological regime stratification of As values. This will provide the data required to relate future results to typical meteorological conditions.
2. Daily sampling should be conducted at two sites (P14 and P15) with dichotomous samplers. All filters should be measured for As and other easily measured major species.
3. This ambient data set should be analyzed by multivariate analysis methods.
4. Particulate samples collected on high As days should be analyzed in more detail for both major and trace species.
5. The data set for high As days should be analyzed by multivariate methods.
6. Additional source sampling is recommended so as to characterize other potential major sources not measured in this feasibility study and to define the variability of source emissions.
7. The multivariate and source sampling results should be combined to determine (a) the primary sources responsible for As variability and (b) develop the most realistic, validated source profiles.
8. Chemical Mass Balance (CMB) methods should be used to quantify the contribution each source makes to fine and coarse particle As levels.
9. The CMB and multivariate analysis results should be compared with general expectations based on meteorology and records of events within the plant.
10. Aerosolizable dust outside the plant boundaries should be sampled, analyzed, and source contributions to As in this dust determined to assess primary sources responsible for indirect contributions.

The above study components are recommended for a basic program which should adequately resolve and quantify source contributions. If this is not adequate for some sources, short term sampling (2 to 4 hours) during special periods or episodes, in addition to the inclusion



of more detailed chemical analyses may be required. Emission inventory scaling might also provide useful insight into source contributions.

## 7.0 REFERENCES

1. Telecon. Whaley, G., Pacific Environmental Services, with White, T., ASARCO, Inc. April 8, 1983. Arsenic material balance for ASARCO-Tacoma.
2. TRW Environmental Engineering Division. Emission Testing of ASARCO Copper Smelter, Tacoma, Washington. EMB Report No. 78-CUS-12. April 1979.
3. TRW Environmental Engineering Division. Emissions Testing of ASARCO Copper Smelter, Tacoma, Washington. EPA Contract No. 68-02-2812, Work Assignment No. 45. August 22, 1979.
4. "Survey of Potential Sources of Fugitive Arsenic Emissions at the ASARCO, Tacoma Smelter". Author and date unknown, provided by J. Nolan, PSAPCA, 1984.
5. "Potential Arsenic Emissions From Road and Field Dust Around ASARCO, Tacoma Smelter". Author and date unknown, provided by J. Nolan, PSAPCA, 1984.
6. Cowherd, C. and P. Englehart, "Emissions of Contaminated Soil Around the ASARCO Tacoma Smelter", Midwest Research Institute draft report, October 3, 1983.
7. "Final Report of Source Tests for Particulate and Arsenic Emissions from Reveratory Furnace Slag Skimming: ASARCO-Tacoma, Copper Smelter", PSAPCA, Seattle, WA., November 19, 1982.
8. Crecelius, E., private communication, April, 1984.
9. "Determination of the Possibility of Arsenic Volatilization from Tacoma Reveratory Slag During Slag Handling", ASARCO report No. 5053, December 27, 1982.
10. "ASARCO Air Curtain Test Project Preliminary Draft Report" from C. Bruffey of Pedco to J. Nolan of PSAPCA, March 22, 1983.
11. "Inorganic Arsenic Emissions from High Arsenic Primary Copper Smelters - Background Information for Proposed Standards", U.S. EPA report No. EPA-450/3-83-009a, April 1983.
12. Friedlander, S.K., Env. Sc. Tech., 7, p. 235.
13. Cooper, J.A. and J. G. Watson, Jr., JAPCA, 1980, 30, p. 1116.
14. Gordon, G.E., Env. Sci & Tech., 1980, 14, p. 792.
15. Lead smelter studies in Kellogg, ID., East Helena, MT., Seattle, WA., and East St. Louis, IL. by NEA, Inc., Beaverton, OR.

16. Cooper, J.A., "Receptor Approach to Quantitative Source Apportionment of Chemical Pollutants in the Environment", NEA course notes for Ontario Ministry of the Environment, November 14, 1983.
17. Houck, J.E., "Dilution Sampling for Chemical Receptor Source Fingerprinting", Proc. 75th Meeting APCA, New Orleans, June 1982.
18. Rhodes, J.R., A. Pradzynski, R.D. Sieberg, T. Furuta, "Application for a Si (Li) Spectrometer to X-Ray Emission Analysis of Thin Specimens", Application of Low Energy X- and Gamma Rays, (C.A. Ziegler ed, pp. 317-334, Gordon & Breach, Publ., 1971.
19. Nielson, K.K., "Matrix Corrections for Energy Dispersive X-Ray Fluorescence Analysis of Environmental Samples With Coherent/Incoherent Scattered X-Rays", Anal. Chem. 48(4), pp. 645-648.
20. Dzubay, T., U.S. EPA, Research Triangle Park, NC, private communication, February 1984.
21. Davies, B.E., ed., Applied Soil Trace Elements, John Wiley & Sons, N.Y., 1980.
22. Braman, R.S., C.C. Foreback, "Methylated Forms of Arsenic in the Environment", Science, 182, pp. 1247-1249, 1973.
23. Kuroda, R., S. Tatsuya, Y. Misu, "Anion-Exchange Behavior and Separation of Metal Ions on DEAE-Cellulose in Oxalic Acid Media". Talanta, 26, pp. 211-214, 1979.
24. Crecelius, E.A., M.H. Bothner, R. Carpenter, "Geochemistries of Arsenic, Antimony, Mercury, and Related Elements in Sediments of Puget Sound", Environmental Sci. & Tech., 9, pp. 325-333, 1975.
25. Andreae, M.O., "Determination of Arsenic Species in Natural Waters", Analytical Chemistry, 49, pp. 820-823, 1977.
26. Leslie, A.C.D., H. Smith, "Napolean Bonaparte's Exposure to Arsenic During 1816", Archives of Toxicology, 41, pp. 163-167, 1978.
27. Jackson, M.L., Soil Chemical Analysis--Advanced Course. A Manual of Methods Useful for Instruction & Research in Soil Chemistry, Phys. Chemistry of Soils, Soil Fertility and Soil Genesis. Revised from original 1956 edition.
28. Cross, J.D., I.M. Dale, A.C.D. Leslie, H. Smith, "Industrial Exposure to Arsenic", Journal of Radioanalytical Chemistry, 48, pp. 197-208, 1979.
29. Jacobs, L.W., J.K. Syers, D.R. Keeney, "Arsenic Sorption by Soils", Soil Sci. Soc. Amer. Proc., 34, pp. 750-754, 1970.
30. Saunders, W.M.H., "Phosphate Retention by New Zealand Soils and Its Relationship to Free Sesquioxides, Organic Matter and Other Soil Properties", New Zealand J. of Agricultural Res., 8, pp. 30-57, 1965.

31. Sisler, H.H., "Phosphorus, Arsenic, Antimony and Bismuth", pp. 106-152, in M.C. Sneed & R.C. Brasted, eds. Comprehensive Inorganic Chemistry, Vol. 5, New York: D. Van Nostrand Co., Inc., 1956.
32. Braman, R.S., D.L. Johnson, C.C. Foreback, J.M. Ammons, and J.L. Bricker, "Separation and Determination of Nanogram Amounts of Inorganic Arsenic and Methyl-Arsenic Compounds", Analytical Chemistry, 49, pp. 621-625, 1977.
33. Crecelius, E.A., "Modification of the Arsenic Specification Technique Using Hydride Generation", Analytical Chemistry, 49, pp. 621-625, 1978.
34. Crecelius, E.A., Battelle-Northwest, Richland, WA, private communication, April 1984.
35. Arsenic, Nat. Academy of Sciences Monograph, Washington, D.C., 1977.
36. Eatough, D.J., N.L. Eatough, M.W. Hill, N.F. Mangelson, J. Ryder, and L.D. Hansen, "The Chemical Composition of Smelter Flue Dusts", Atmospheric Environment, 13, pp. 489-506, 1979.
37. Eatough, D.J., J.J. Christense, N.L. Eatough, M.W. Hill, T.D. Major, N.F. Mangelson, M.E. Post, J.F. Ryder, and L.D. Hansen, "Sulfur Chemistry in a Copper Smelter Plume", Atmospheric Environment, 13, pp. 1001-1015, 1982.
38. Eatough, D.J., F.E. Richter, N.L. Eatough, L.D. Hansen, "Sulfur Chemistry in Smelter and Power Plant Plumes in the Western U.S.", Atmospheric Environment, 15, pp. 2241-2253, 1981.
39. Cooper, J.A., R.T. DeCesar, C.A. Frazier, J.E. Houck, and J.F. Mohan, "Determination of Source Contributions to Air Particulate Lead and Cadmium Levels in Kellog, Idaho Using the Receptor Model", Final Report, NEA, Inc., Beaverton, OR, December 10, 1981.

Table 1

List of Potential Arsenic Sources  
and Estimated Emission Rates (kg/hr)<sup>11</sup>

Process Ducted Emissions

- Herreshoff Roasters (0.4)
- Reverbatory Furnaces (9.5)
- Converters (0.04)
- Anode Furnace (0.02)
- Arsenic Plant (7.3)

Fugitive Emissions

- Roaster
  - Chargine
  - Leakage
  - Hot calcine discharge and transfer (0.03)
- Smelting Furnace
  - Charging
  - Leakage
  - Matte Tapping (0.5)
  - Slag Tapping (0.03)
  - Converter slag return (0.01)
- Converters (14)
  - Charging
  - Blowing
  - Skimming
  - Holding
  - Pouring slag and blister
  - Leakage
- Anode Furnace (0.08)
  - Charging
  - Blowing
  - Holding
  - Pouring
- Miscellaneous (0.3)
  - Dust handling and transfer
  - Ladles
  - Slag dumping
  - Stack cleaning
  - Flue pulling
- Arsenic Building (0.6)

Indirect Resuspension

Table 2

Summary of Sampling Data for Process Emissions Sampled  
at the ASARCO - Tacoma Copper Smelter

Filter ID	Run No.	Source Description	Filter Type	Particle Size ( $\mu$ )	Sample Time Start/Stop	Vol. ( $m^3$ )	Sample Duration	Temperature $^{\circ}C$			Deposit Mass (mg)
								Flue	Ambient	D. Cham.	
MF893	1	Slag skim, reverb. furnace	T	< 2.5	27-20:52/27-21:10	0.300	18 min.	-	-	-	21.779
MC894	1	Slag skim, reverb. furnace	T	> 2.5	27-20:52/27-21:10	0.300	18 min.	-	-	-	3.294
ML838	1	Slag skim, reverb. furnace	T	TSP	27-20:52/27-21:10	0.658	18 min.				63.231
MF863	2	Slag skim, reverb. furnace	T	< 2.5	27-23:20/27-23:36	0.267	16 min.				9.242
MC864	2	Slag skim, reverb. furnace	T	> 2.5	27-23:20/27-23:36	0.267	16 min.				1.330
ML841	2	Slag skim, reverb. furnace	T	TSP	27-23:20/27-23:36	0.656	16 min.				28.261
MF867	3	Slag skim, reverb. furnace	T	< 2.5	28-00:04/28-00:28	0.401	24 min.				13.733
MC868	3	Slag skim, reverb. furnace	T	> 2.5	28-00:04/28-00:28	0.401	24 min.				2.071
ML839	3	Slag skim, reverb. furnace	T	TSP	28-00:04/28-00:28	0.984	24 min.				44.451
MF871	4	Slag skim, reverb. furnace	T	< 2.5	28-00:50/28-01:06	0.267	16 min.				10.044
MC870	4	Slag skim, reverb. furnace	T	> 2.5	28-00:50/28-01:06	0.267	16 min.				1.490
ML835	4	Slag skim, reverb. furnace	T	TSP	28-00:50/28-01:06	0.666	16 min.				33.441
MF897	1	Convertor #4, secondary hood	T	< 2.5	27-20:48/27-20:58	0.167	10 min.				0.093
MC898	1	Convertor #4, secondary hood	T	> 2.5	27-20:48/27-20:58	0.167	10 min.				0.024
ML836	1	Convertor #4, secondary hood	T	TSP	27-20:48/27-20:58	0.455	10 min.				38.427
MF895	2	Convertor #4, secondary hood	T	< 2.5	27-21:01/27-21:38	0.618	37 min.				3.774
MC896	2	Convertor #4, secondary hood	T	> 2.5	27-21:01/27-21:38	0.618	37 min.				0.487
ML840	2	Convertor #4, secondary hood	T	TSP	27-21:01/27-21:38	1.629	37 min.				58.342
MF865	3	Convertor #4, secondary hood	T	< 2.5	27-23:13/28-00:18	1.086	65 min.				8.468
MC866	3	Convertor #4, secondary hood	T	> 2.5	27-23:13/28-00:18	1.086	65 min.				1.121
ML842	3	Convertor #4, secondary hood	T	TSP	27-23:13/28-00:18	2.054	65 min.				> 115
MF869	4	Convertor #4, secondary hood	T	< 2.5	28-00:30/28-01:29	0.985	59 min.				2.121
MC872	4	Convertor #4, secondary hood	T	> 2.5	28-00:30/28-01:29	0.985	59 min.				0.238
ML837	4	Convertor #4, secondary hood	T	TSP	28-00:30/28-01:29	1.711	59 min.				18.101
MF873	*1	#1 Brick Flue	T	< 2.5	27-19:46/28-09:38		13.83 hrs.	85	10	16	7.170
MC874	*1	#1 Brick Flue	T	> 2.5	27-19:46/28-09:38		13.83 hrs.	85	10	16	1.910
MF875	*1	#1 Brick Flue	T	< 2.5	27-19:46/28-09:38		13.83 hrs.	85	10	16	6.269
MC876	*1	#1 Brick Flue	T	> 2.5	27-19:46/28-09:38		13.83 hrs.	85	10	16	1.839
MF877	*2	#1 Brick Flue	T	< 2.5	28-10:42/28-19:31		8.82 hrs.	82	11	16	5.655
MC878	*2	#1 Brick Flue	T	> 2.5	28-10:42/28-19:31		8.82 hrs.	82	11	16	1.302
MF879	*2	#1 Brick Flue	T	< 2.5	28-10:42/28-19:31		8.82 hrs.	82	11	16	6.225
MC880	*2	#1 Brick Flue	T	> 2.5	28-10:42/28-19:31		8.82 hrs.	82	11	16	1.460
MF881	*3	#1 Brick Flue	T	< 2.5	28-19:57/29-08:51		12.90 hrs.	85	7	13	6.744
MC882	*3	#1 Brick Flue	T	> 2.5	28-19:57/29-08:51		12.90 hrs.	85	7	13	1.728
MF883	*3	#1 Brick Flue	T	< 2.5	28-19:57/29-08:51		12.90 hrs.	85	7	13	6.358
MC884	*3	#1 Brick Flue	T	> 2.5	28-19:57/29-08:51		12.90 hrs.	85	7	13	1.539
None	*1	DSS Inlet, #1 Brick Flue	8X10 glass		27-19:46/28-9:38		13.83 hrs.	85	10	16	
None	*1	DSS Outlet, #1 Brick Flue	8X10 glass		27-19:46/28-9:38		13.83 hrs.	85	10	16	
MF897	*2	DSS Outlet, #1 Brick Flue	8X10 glass		28-10:42/28-19:31		8.82 hrs.	82	11	16	
None	*2	DSS Inlet, #1 Brick Flue	8X10 glass		28-10:42/28-19:31		8.82 hrs.	82	11	16	
MF898	*3	DSS Outlet, #1 Brick Flue	8X10 glass		28-19:57/29-8:51		12.90 hrs.	85	7	13	
None	*3	DSS Inlet, #1 Brick Flue	8X10 glass		28-19:57/29-8:51		12.90 hrs.	85	7	13	
None	3	Probe Impact Sample			3/27/84-3/29/84						

\*Samples collected with NEA's size-segregating dilution sampler.

T = teflon

Table 3

Summary of Resuspension Data for Bulk Source Samples  
Collected from the ASARCO - Tacoma Copper Smelter

Sample No.	Sample Description	Type Sampler	Filter ID	Net Deposit (mg)	Fine to Coarse Ratio <sup>a</sup>	Comments
1	Slag dump composite	Dichot	CB282	1.593	0.040	
		Dichot	FB283	0.110	0.040	
2	Slag dump fines	Lo-vol	LB332	1.134	NA	< 7.5 $\mu$ , > 38 $\mu$
3	Martin Mill weighing floor	Dichot	CB292	1.179	0.019	
		Dichot	FB293	0.124	0.019	
4	Roadway by fine ore bins	Dichot	CB284	1.023	0.10	
		Dichot	FB285	0.136	0.10	
5	Roadway by Sample Bldg.	Dichot	CB286	1.015	0.097	deposit uneven
		Dichot	FB287	0.137	0.097	
6	As Baghouse concrete pad	Dichot	CB300	2.564	0.034	not sieved
		Dichot	FB301	0.201	0.034	not sieved
7	Road dust: 52nd & Bennett	TSP	1B339			not enough material to resusp.
8	Road dust: 49th & Baltimore	Dichot	CB274	1.168	0.046	
		Dichot	FB275	0.203	0.046	
9	RR track, south gate	Dichot	CB306	0.988	0.11*	
		Dichot	FB707	0.111	0.11*	
10	#1 flue dust	Dichot	CB298	1.602	0.016	not sieved
		Dichot	FB299	0.037	0.016	not sieved
11	Herreshoff Roaster calcine	Dichot	CB294	0.335	0.062	deposit splotchy
		Dichot	FB295	0.154	0.062	deposit splotchy
12	Lepanto Cu concentrate	Lo-vol	LB333	1.336	NA	<75, >38 $\mu$
13	SO <sub>2</sub> Cottrell dust	Dichot	CB290	1.068	0.033	not sieved
		Dichot	FB291	0.075	0.033	not sieved
14	Herreshoff Roaster charge	Dichot	CB296	0.846	0.050	deposit uneven
		Dichot	FB297	0.160	0.050	deposit uneven
15	As Plant product	Dichot	CB302	0.690	0.055	not sieved
		Dichot	FB303	0.038	0.055	not sieved

<sup>a</sup>Fine < 2.5  $\mu$ m; Coarse > 2.5  $\mu$ m, 15  $\mu$ m. Ratio based on intermediate loadings. Additional mass added to fine filter

\*Large uncertainty in this ratio because mass on coarse filter was not reproducible

Table 4

Average Fine to Coarse Particle Ratios After  
Correcting for Fine Particles Deposited on Coarse Particle Filter

<u>Source</u>	<u>F/C Ratio</u>
Reverbatory Furnace Slag Skimming	27
Converter Secondary Hood	(254 ± 437)
No. 1 Brick Flue Gas Stream	(7.2)
Herreshoff Roaster Charge	0.050
Herreshoff Roaster Calcine	0.062
Road Dust 48th and Baltimore	0.046
Railroad Track Dust	(0.11)**
Slag Dump Composite	0.04
Slag Dump Fine	<< 0.01
SO <sub>2</sub> Cottrell Dust	0.033
No. 1 Flue Dust	0.016
As Baghouse Dust	0.034
As Plant Product	0.055
Roadway Dust by Fine Ore Bin	0.10
Roadway Dust by Sample Bldg.	0.097
Martin Mill Weighing Floor	0.019
Lepanto Copper Ore Concentrate	<< 0.01

\*\* Large uncertainty in this ratio because mass on coarse filter was not reproducible. This ratio is thought to be an upper limit.



Table 5

Percent Elemental Composition of  
Herreshoff Roaster Charge and Calcine

Element	Roaster		Calcine	
	Coarse	Fine	Coarse	Fine
	CB296	FB297	CM294	FB295
Al	2.1 ± .4	4.3 ± .5	2.4 ± .2	6.3 ± .6
Si	7.2 ± .8	12.0 ± 1.0	4.8 ± .5	13.5 ± 1.2
S	10.4 ± 1.2	12.4 ± 1.1	8.1 ± .3	9.8 ± 0.9
Cl	< 0.1	< 0.1	< 0.1	< 0.1
K	0.39 ± .09	0.68 ± .07	0.42 ± .08	1.01 ± .10
Ca	1.13 ± .08	0.78 ± .08	1.62 ± .11	2.0 ± .17
Ti	0.16 ± .03	0.19 ± .02	0.16 ± .04	0.26 ± .05
V	< 0.03	< 0.03	< 0.04	< 0.05
Cr	0.036 ± .012	0.05 ± .01	0.04 ± .02	0.066 ± .015
Mn	0.053 ± .015	0.076 ± .010	0.081 ± .018	0.137 ± .015
Fe	10.5 ± .7	8.9 ± 0.7	13.0 ± .6	18.6 ± 1.5
Ni	0.11 ± .01	0.15 ± .03	< .08	0.11 ± .05
Cu	18.5 ± 2.0	18.9 ± 1.5	18.4 ± 1.9	18.6 ± 1.5
Zn	0.77 ± .09	0.85 ± .10	1.02 ± .08	1.09 ± .12
As	6.5 ± .4	8.8 ± 0.7	3.7 ± .6	4.2 ± .4
Se	0.04 ± .02	0.04 ± .02	< 0.03	< .05
Br	< 0.2	< 0.2	< 0.2	< .3
Rb	< 0.01	< 0.01	< 0.05	< 0.04
Sr	< 0.03	0.03 ± .01	< 0.04	.05 ± .02
Y	< 0.02	< 0.02	< 0.04	< 0.03
Mo	0.10 ± .02	< .05	0.12 ± .04	0.16 ± .05
Ag	0.10 ± .02	0.16 ± .05	0.042 ± .010	< 0.2
Cd	0.045 ± .015	< 0.1	< 0.02	< 0.2
In	< 0.03	< 0.1	< 0.02	< 0.2
Sn	< 0.05	< 0.1	< 0.02	< 0.2
Sb	0.25 ± .05	0.2 ± 0.1	0.076 ± .021	0.34 ± .16
Te	< 0.05	< 0.1	< 0.1	< 0.2
Hg	< 0.04	< 0.04	< 0.04	< 0.1
Pb	1.90 ± .12	2.3 ± 0.2	1.75 ± .10	2.13 ± .18
Bi	(0.3 ± .1)	(0.3 ± .1)	(0.06 ± .03)	(0.3 ± .1)
Mass (µg)	846	160	335	154
F/C	0.050	0.050	0.062	0.062

Table 6

Percent Elemental Composition of Particles  
in Road and Railroad Track Dust

Element	49B Road Dust		52B R.Dust Total MB339*	Railroad Track South Gate		
	Coarse CB274	Fine FB275		Coarse CB306 <sup>a</sup>	Fine FB307 <sup>b</sup>	Coarse CB306 <sup>c</sup>
Al	5.7 ± .3	10.7 ± 0.8		0.2 ± 0.1	2 ± 0.5	1.3
Si	23.6 ± 1.5	35 ± 0.4		1.5 ± 0.3	10.5 ± 1.3	9.8
S	0.6 ± .1	1.2 ± 0.2		0.13 ± 0.08	1.5 ± 0.5	0.85
Cl	< 0.04	0.2 ± 0.1		< 0.05	< 0.1	< 0.33
K	0.62 ± .05	0.87 ± 0.07		0.05 ± 0.02	0.3 ± .1	0.33
Ca	1.40 ± .09	1.53 ± 0.13		0.11 ± .04	0.7 ± .2	0.72
Ti	0.39 ± .03	0.45 ± 0.05		0.03 ± .02	0.12 ± .05	0.20
V	0.020 ± .007	0.027 ± .009		< 0.01	0.05 ± .02	< 0.065
Cr	0.032 ± .006	0.040 ± .006		< 0.01	0.05 ± 0.01	< 0.065
Mn	0.068 ± .007	0.094 ± .010		0.024 ± .004	0.12 ± .02	0.16
Fe	6.3 ± .3	7.5 ± .6	(0.39)	2.15 ± .15	11.6 ± 1.4	14.0
Ni	0.022 ± .005	0.034 ± .008		0.010 ± .002	< 0.05	0.065
Cu	1.13 ± .06	1.29 ± 0.10	(0.17)	1.10 ± .06	7.0 ± 0.8	7.2
Zn	0.192 ± .012	0.22 ± 0.020		0.30 ± .02	2.0 ± 0.2	2.0
As	2.47 ± .15	1.80 ± 0.15	≅ 2.0	2.02 ± .12	13.2 ± 1.5	≅ 13.2
Se	< 0.02	< 0.02		< 0.02	< 0.04	< 0.13
Br	< 0.1	< 0.15		< 0.15	< 0.6	< 0.98
Rb	< 0.01	< 0.01		< 0.01	< 0.03	< 0.065
Sr	0.022 ± .005	0.020 ± .008		< 0.01	< 0.04	< 0.065
Y	< 0.005	< 0.010		< 0.01	< 0.04	< 0.065
Mo	0.025 ± .007	< 0.030		< 0.02	< 0.02	< 0.13
Ag	< 0.02	< 0.04		< 0.03	< 0.08	< 0.20
Cd	< .04	< 0.1		< 0.1	< 0.4	< 0.65
In	< .03	< 0.1		< 0.05	< 0.2	< 0.33
Sn	< .03	< 0.1		< 0.05	0.3 ± 0.1	< 0.33
Sb	0.07 ± .02	< 0.1	(0.04)	0.084 ± .028	0.3 ± 0.1	0.55
Te	< 0.02	< 0.1		< 0.05	< 0.2	< 0.33
Hg	0.023 ± .008	< 0.05		< .03	< 0.1	< 0.20
Pb	0.46 ± .03	1.14 ± .09	(0.09)	1.02 ± .05	6.5 ± 0.7	6.7
Bi	(< .05)	(< 0.1)		(0.16 ± .05)	(1.2 ± 0.3)	1.0
Mass (µg)	1168	203	-	988**	111	
F/C	0.046	0.046	-	0.11**	0.11**	

<sup>a</sup>T1 = 0.04%<sup>b</sup>T1 = 0.20%<sup>c</sup>Normalized Sb ≅ 13.2

\*Insufficient material was collected for resuspension and the glass fiber filter was cut in half in the field so a deposit mass could not be determined. All numbers have been normalized to an arsenic value of 2.0.

\*\*Large uncertainty in this ratio because mass on coarse filter was not reproducible and particles would not stick to filter.

Table 7  
Percent Elemental Composition of Slag

Element	Slag Dump Composite		Slag Dump Fine Total LB332 <sup>a</sup>
	Coarse CB282 <sup>b</sup>	Fine FB283	
Al	1.8 ± 0.2	3.1 ± 0.6	3.8 ± 0.2
Si	14.1 ± 0.9	15.8 ± 1.6	21.7 ± 1.2
S	0.58 ± .09	1.5 ± 0.3	0.69 ± 0.05
Cl	0.51 ± .04	0.82 ± 0.12	0.17 ± 0.02
K	0.42 ± .03	0.40 ± .06	0.79 ± 0.05
Ca	3.6 ± .2	2.3 ± .3	5.3 ± 0.3
Ti	0.30 ± .05	0.21 ± 0.05	0.24 ± 0.02
V	0.04 ± .01	0.04 ± .01	0.02 ± .01
Cr	0.11 ± .02	0.08 ± .02	0.07 ± .01
Mn	0.13 ± .02	0.10 ± .02	0.24 ± .02
Fe	21.6 ± 1.4	14.1 ± 1.5	5.6 ± .3
Ni	0.041 ± .005	0.043 ± 0.015	0.020 ± .003
Cu	1.96 ± 0.10	2.5 ± 0.3	0.255 ± .015
Zn	1.74 ± 0.09	1.62 ± 0.17	0.275 ± .016
As	1.88 ± .12	2.5 ± 0.3	0.124 ± .013
Se	< 0.01	< 0.01	< 0.01
Br	< 0.1	< 0.1	< 0.1
Rb	< 0.01	< 0.01	< 0.02
Sr	0.019 ± .004	< 0.03	0.023 ± .005
Y	< 0.01	< 0.03	< 0.01
Mo	0.100 ± .015	< 0.05	< 0.03
Ag	< 0.02	< 0.08	< 0.03
Cd	0.05 ± .01	< 0.3	< 0.05
In	< 0.04	< 0.3	< 0.04
Sn	< 0.06	< 0.3	< 0.04
Sb	0.19 ± 0.03	< 0.3	< 0.04
Te	< 0.04	< 0.3	< 0.04
Hg	< 0.03	< 0.2	< 0.03
Pb	0.89 ± .08	1.28 ± .14	0.141 ± .012
Bi	(= .05)	(< 0.2)	(< 0.1)
Mass (µg)	1593	110	1134
F/C	0.04	0.04	

<sup>a</sup>None of the bulk material sampled passed through the 400 mesh (38 µm) sieve. The material in the size range from 38 µm to 78 µm was resuspended and sampled with a low-volume TSP sampler.

<sup>b</sup>Tl = 0.1%

Table 8

## Percent Elemental Composition of High Arsenic Bulk Samples

Element	SO <sub>2</sub> Cottrell Dust		No. 1 Flue Dust		As Baghouse Pad		As Plant Product	
	Coarse CB290	Fine FB291	Coarse CB298	Fine FB299	Coarse CB300	Fine FB301	Coarse CB302	Fine FB303
Al	< 0.5	< 0.5	< 0.8	< 0.5	< 1.0	< 1.0	< 1.0	< 1.0
Si	< 1.0	< 1.0	< 1.0	< 2.0	< 1.0	< 2.0	< 1.0	< 1.0
S	< 2.0	< 2.0	< 2.0	< 3.0	< 0.5	< 2.0	0.8 ± .2	< 1.0
Cl	< 0.4	< 0.4	< 0.4	< 0.5	< 0.1	< 0.2	< 0.1	< 0.2
K	< 0.2	< 0.2	< 0.4	< 0.4	< 0.2	< 0.5	< 0.1	< 0.3
Ca	< 0.6	< 0.6	< 0.5	< 0.8	< 0.4	< 0.3	< 0.2	< 0.2
Ti	< 0.05	< 0.1	< 0.07	< 0.1	< 0.05	< 0.05	< .05	< 0.05
V	< 0.02	< 0.02	< 0.02	< 0.05	0.012 ± .005	< 0.02	< .01	< 0.02
Cr	< 0.01	< 0.01	0.02 ± .01	< 0.07	0.016 ± .010	< 0.02	< .01	< 0.02
Mn	< 0.01	< 0.02	0.02 ± .01	< 0.04	0.02 ± .01	< 0.02	< .01	< 0.02
Fe	0.3 ± .1	0.36 ± .06	2.9 ± 0.2	1.08 ± .25	2.11 ± .10	2.2 ± .2	2.67 ± .15	0.54 ± .20
Ni	< 0.05	0.042 ± 0.014	< 0.05	< 0.05	< 0.04	< 0.04	0.03 ± .01	< 0.02
Cu	0.30 ± 0.05	0.28 ± 0.04	5.8 ± .3	4.0 ± 0.8	2.11 ± .10	2.5 ± 0.2	3.6 ± .2	0.38 ± .12
Zn	1.4 ± 0.1	0.95 ± 0.13	1.9 ± 0.1	1.7 ± 0.4	0.38 ± .02	0.52 ± .04	0.41 ± .02	0.14 ± 0.06
As	26 ± 3	8.6 ± 1.5	36 ± 3	31 ± 6	64 ± 3	26 ± 2	51 ± 3	4.0 ± 1.0
Se	< 0.1	< 0.1	< 0.1	< 0.1	0.11 ± .02	0.22 ± 0.02	0.18 ± .02	< 0.3
Br	< 0.4	< 0.5	< 0.4	< 0.5	< 0.3	< 0.4	< 0.3	< 0.3
Rb	< 0.1	< 0.04	< 0.1	< 0.1	< 0.05	< 0.1	< 0.05	< 0.05
Sr	< 0.1	< 0.05	< 0.1	< 0.1	< 0.02	< 0.1	< 0.05	< 0.05
Y	< 0.1	< 0.06	< 0.1	< 0.1	< 0.05	< 0.1	< 0.05	< 0.05
Mo	< 0.05	< 0.1	0.145 ± .011	< 0.2	0.03 ± .01	0.05 ± 0.02	0.03 ± .01	< 0.3
Ag	< 0.05	< 0.2	< 0.05	< 0.4	< 0.05	< 0.2	< 0.02	< 0.4
Cd	< 0.05	< 0.2	< 0.05	< 0.4	< 0.05	< 0.2	0.04 ± .01	< 0.4
In	< 0.05	< 0.3	< 0.05	< 0.5	< 0.06	< 0.2	< 0.02	< 0.5
Sn	< 0.6	1.0 ± 0.2	< 0.06	< 0.5	< 0.07	< 0.2	< 0.02	< 0.5
Sb	0.89 ± 0.06	1.0 ± 0.2	1.14 ± .08	2.4 ± 0.1	2.15 ± .15	6.8 ± .6	2.14 ± .15	< 0.6
Te	< 0.06	< 0.3	< 0.06	< 0.6	< 0.1	< 0.2	< 0.02	< 0.6
Hg	< 0.2	0.06 ± .03	< 0.2	< 0.2	0.21 ± .03	0.15 ± 0.03	0.19 ± 0.04	< 0.3
Pb	37 ± 3	28 ± 3	6.5 ± .3	7.5 ± 1.5	1.26 ± .06	0.20 ± .04	1.97 ± .08	0.50 ± .24
Bi	(4 ± 1)	(4 ± 1)	(1.2 ± .4)	(< 1)	(0.04 ± .01)	(1.2 ± .2)	(0.5 ± 0.1)	(< 1)
Mass (µg)	778	59	1578	26	2361	195	551	19
F/C	0.033	0.033	0.016	0.016	0.034	0.034	0.055	0.055

Table 9  
Percent Elemental Composition of Settled Dust  
Collected Within the Plant and the Ore Concentrate

Element	Roadway Dust by FOB		Roadway Dust by Sample Bldg.		Martin Mill Weighing Floor		Lepanto Copper Concentrate
	Coarse CB284	Fine FB285	Coarse CB286 <sup>b</sup>	Fine FB287 <sup>c</sup>	Coarse CB292	Fine FB293	Total LB333
Al	2.5 ± 0.2	5.9 ± 0.6	2.4 ± 0.2	4.4 ± .4	2.0 ± 0.2	5.5 ± 0.6	0.27 ± 0
Si	6.4 ± 0.3	12.1 ± 1.2	7.4 ± 0.4	11.4 ± 1.2	7.6 ± 0.4	14.1 ± 1.5	1.47 ± 0.08
S	11.8 ± 0.7	12.5 ± 1.2	6.9 ± 0.4	6.9 ± 0.8	13.4 ± 0.7	13.2 ± 1.4	7.8 ± 0.4
Cl	< 0.1	< 0.1	< 0.1	< 0.1	< 0.1	< 0.1	< 0.1
K	0.42 ± 0.02	0.92 ± .09	0.31 ± 0.2	0.60 ± .07	0.32 ± .02	0.71 ± .08	0.11 ± .01
Ca	0.72 ± .05	0.87 ± .09	3.4 ± 0.2	4.9 ± .5	1.39 ± .08	1.00 ± .10	0.36 ± 0.02
Ti	0.20 ± 0.02	0.26 ± .03	0.18 ± .01	0.22 ± .03	0.18 ± .03	0.18 ± .03	0.12 ± 0.01
V	< 0.04	< 0.03	< 0.03	< 0.03	< 0.03	< 0.03	< 0.03
Cr	0.060 ± .010	0.083 ± .025	0.054 ± .009	0.057 ± .010	0.04 ± .01	0.05 ± .01	0.025 ± 0.10
Mn	0.076 ± .008	0.081 ± .015	0.064 ± .008	0.084 ± .012	0.048 ± .006	0.05 ± .01	0.036 ± .15
Fe	17.9 ± 0.9	17.3 ± 1.5	11.8 ± 0.6	11.1 ± 1.0	10.9 ± 0.6	8.0 ± .8	13.2 ± 0.7
Ni	< 0.05	< 0.1	< 0.1	0.11 ± 0.03	< 0.1	< 0.1	< 0.1
Cu	18.7 ± 1.0	17.2 ± 1.5	13.0 ± 0.7	12.5 ± 1.2	18.2 ± 1.0	15.8 ± 1.5	17.7 ± 0.9
Zn	1.12 ± .09	1.4 ± .2	1.05 ± .08	1.47 ± .14	0.56 ± .08	0.37 ± .07	0.55 ± 0.07
As	1.99 ± .15	4.4 ± .5	2.4 ± 0.2	3.9 ± 0.5	6.9 ± .4	6.5 ± .6	7.0 ± 0.4
Se	< 0.02	< 0.02	< 0.02	< 0.4	0.04 ± .01	< 0.4	0.04 ± .01
Br	< 0.1	< 0.1	< 0.1	< 0.2	< 0.2	< 0.2	< 0.2
Rb	< 0.01	< 0.02	< 0.02	< 0.02	< 0.02	< 0.02	< 0.02
Sr	0.014 ± .005	< 0.02	< 0.02	< 0.02	0.023 ± .005	0.04 ± 0.02	< 0.02
Y	< 0.01	< 0.02	< 0.02	< 0.03	< .03	< 0.03	< 0.03
Mo	0.32 ± 0.02	0.36 ± .06	0.16 ± .02	0.11 ± .05	< 0.05	< 0.08	< 0.05
Ag	0.052 ± .010	< 0.1	0.08 ± .02	0.14 ± .06	0.06 ± .01	< 0.2	< 0.04
Cd	0.08 ± .03	< 0.2	0.10 ± .03	< 0.15	< 0.03	< 0.2	< 0.05
In	< 0.04	< 0.2	< 0.05	< 0.1	< 0.03	< 0.2	< 0.05
Sn	< 0.04	< 0.2	0.08 ± .02	< 0.1	0.07 ± .03	< 0.2	< 0.05
Sb	0.068 ± .028	0.3 ± 0.2	0.15 ± 0.05	< 0.1	0.22 ± .03	< 0.2	0.20 ± 0.04
Te	< 0.04	< 0.1	< 0.1	< 0.1	< 0.04	< 0.2	< 0.05
Hg	< 0.02	< 0.05	< 0.05	< 0.05	< 0.05	< 0.1	< 0.05
Pb	1.82 ± .10	4.6 ± 0.4	3.1 ± 0.2	5.8 ± .6	0.39 ± .02	1.07 ± .12	0.21 ± 0.02
Bi	(0.4 ± 0.1)	(0.7 ± .2)	(0.6 ± .2)	(0.7 ± 0.2)	(0.16 ± .04)	(< 0.3)	(0.07 ± 0.01)
Mass(μg)	1023	136	1015	137	1179	124	1336
F/C	0.10	0.10	0.097	0.097	0.019	0.019	-

<sup>a</sup>None of the bulk sample passed through the 400 mesh (< 38 μm) sieve. Particles in the size range from 38 μm to 78 μm was resuspended and sampled with a low-volume TSP sampler.

<sup>b</sup>T1 = 0.1%

<sup>c</sup>T1 = 0.3%

Table 10

Percent Elemental Composition of Emission from Number 1  
Brick Flue: Fine Fraction ( < 2.5  $\mu$ m)

Element	Sample Identification				
	MF875	MF877	MF879	MF883	Mean $\pm$ SD
Al	< 0.2	< 0.2	< 0.2	< 0.2	< 0.2
Si	< 0.2	< 0.2	< 0.2	< 0.2	< 0.2
S	< 2.0	< 2.0	< 2.0	< 2.0	< 2.0
Cl	< 0.3	< 0.3	< 0.3	< 0.3	< 0.3
K	< 0.5	< 0.5	< 0.5	< 0.5	< 0.5
Ca	< 0.8	< 0.8	< 0.8	< 0.8	< 0.8
Ti	< 0.1	< 0.1	< 0.1	< 0.1	< 0.1
V	.015 $\pm$ .003	0.016 $\pm$ .005	0.016 $\pm$ .006	0.016 $\pm$ .003	0.016 $\pm$ 0.00050
Cr	.013 $\pm$ 0.003	0.014 $\pm$ .004	0.015 $\pm$ .004	0.014 $\pm$ .003	0.014 $\pm$ 0.00082
Mn	< 0.01	0.010 $\pm$ .005	0.014 $\pm$ .008	< 0.01	0.0085 $\pm$ 0.0044
Fe	0.28 $\pm$ .02	0.28 $\pm$ 0.02	0.32 $\pm$ 0.02	0.28 $\pm$ 0.02	0.29 $\pm$ 0.020
Ni	0.03 $\pm$ .01	0.04 $\pm$ .01	0.05 $\pm$ .02	0.04 $\pm$ .02	0.040 $\pm$ 0.0082
Cu	2.8 $\pm$ 0.2	3.2 $\pm$ 0.2	2.7 $\pm$ .2	3.2 $\pm$ .2	3.0 $\pm$ 0.26
Zn	3.2 $\pm$ 0.2	3.7 $\pm$ 0.3	6.3 $\pm$ .3	3.7 $\pm$ .2	4.2 $\pm$ 1.4
As	21.2 $\pm$ 1.8	26.4 $\pm$ 1.7	26.4 $\pm$ 1.7	23.1 $\pm$ 1.6	24 $\pm$ 2.6
Se	< 0.1	< 0.1	< 0.1	< 0.1	< 0.1
Br	< 0.3	< 0.3	< 0.3	< 0.3	< 0.3
Rb	< 0.1	< 0.1	< 0.1	< 0.1	< 0.1
Sr	< 0.1	< 0.1	< 0.1	< 0.1	< 0.1
Y	< 0.1	< 0.1	< 0.1	< 0.1	< 0.1
Mo	0.11 $\pm$ .02	0.09 $\pm$ .02	0.11 $\pm$ .02	0.09 $\pm$ 0.02	0.10 $\pm$ 0.012
Ag	0.13 $\pm$ .04	0.11 $\pm$ .02	0.13 $\pm$ .03	0.10 $\pm$ .02	0.12 $\pm$ 0.015
Cd	0.72 $\pm$ .24	0.40 $\pm$ .05	0.40 $\pm$ .08	0.53 $\pm$ .07	0.51 $\pm$ .15
In	0.02 $\pm$ .01	0.02 $\pm$ .01	0.03 $\pm$ .01	0.02 $\pm$ .01	0.023 $\pm$ 0.0050
Sn	0.34 $\pm$ .12	0.48 $\pm$ .10	0.42 $\pm$ .09	0.36 $\pm$ .09	0.40 $\pm$ 0.063
Sb	6.6 $\pm$ 0.6	6.0 $\pm$ .4	6.1 $\pm$ .5	5.2 $\pm$ 0.4	6.0 $\pm$ 0.58
Te	0.20 $\pm$ .05	0.16 $\pm$ .04	0.16 $\pm$ .04	0.14 $\pm$ .04	0.17 $\pm$ 0.025
Hg	0.2 $\pm$ 0.1	< 0.2	< 0.2	< 0.2	< 0.2
Pb	18.6 $\pm$ 1.0	17.9 $\pm$ 0.9	17.6 $\pm$ 0.9	19.7 $\pm$ 1.0	18 $\pm$ 0.93
Bi	0.5 $\pm$ 0.1	0.4 $\pm$ 0.1	0.3 $\pm$ 0.1	0.4 $\pm$ 0.1	0.40 $\pm$ 0.082
Mass ( $\mu$ g)	6269	5655	6225	6358	
F/C	5.5	8.4	8.1	7.6	7.2 <sup>a</sup>

<sup>a</sup>All values included

Table 11

Percent Elemental Composition of Emission from Number 4 Converter  
Secondary Hood: Fine Fraction ( < 2.5  $\mu\text{m}$ )

Element	Sample Identification				
	MF869	MF897	MF895	MF865	Mean $\pm$ SD
Al	< 0.2	< 0.2	< 0.2	< 0.2	< 0.2
Si	< 0.2	< 0.2	< 0.2	< 0.2	< 0.2
S	< 2	< 2	< 2	< 2	< 2
Cl	< 0.2	< 0.2	< 0.2	< 0.2	< 0.2
K	< 0.2	< 0.2	< 0.2	< 0.2	< 0.2
Ca	< 0.2	< 0.5	< 0.4	< 0.6	< 0.4
Ti	< 0.02	< 0.2	< 0.1	< 0.05	< 0.1
V	< 0.01	< 0.03	< 0.03	< 0.01	< 0.02
Cr	< 0.01	< 0.03	< 0.02	< 0.02	< 0.02
Mn	< 0.01	< 0.03	0.02 $\pm$ 0.01	< 0.02	< 0.02
Fe	0.135 $\pm$ .010	0.50 $\pm$ 0.15	0.33 $\pm$ 0.05	.08 $\pm$ .02	0.26 $\pm$ 0.19
Ni	< 0.02	< 0.03	0.04 $\pm$ 0.01	< .04	< 0.03
Cu	0.41 $\pm$ .02	0.53 $\pm$ 0.10	2.8 $\pm$ 0.2	0.66 $\pm$ .05	1.1 $\pm$ 1.1
Zn	1.06 $\pm$ .08	1.76 $\pm$ .25	6.4 $\pm$ 0.4	1.09 $\pm$ .08	2.6 $\pm$ 2.6
As	18.7 $\pm$ 1.5	41 $\pm$ 6	17.8 $\pm$ 2.6	29 $\pm$ 2	26 $\pm$ 11
Se	< 0.2	< 0.2	< 0.2	< 0.2	< 0.2
Br	< 0.2	< 0.2	< 0.3	< 0.2	< 0.2
Rb	< 0.04	< 0.08	< 0.06	< 0.06	< 0.06
Sr	< 0.02	< 0.06	< 0.05	< 0.06	< 0.05
Y	< 0.04	< 0.15	< 0.09	< 0.10	< 0.09
Mo	0.04 $\pm$ 0.02	< 0.15	< 0.15	< 0.04	< 0.1
Ag	0.08 $\pm$ .03	0.8 $\pm$ 0.3	0.12 $\pm$ 0.04	0.04 $\pm$ .03	0.26 $\pm$ 0.36
Cd	0.20 $\pm$ .06	1.9 $\pm$ 0.4	< 0.1	0.25 $\pm$ .08	0.60 $\pm$ 0.87
In	< 0.01	0.30 $\pm$ 0.10	0.10 $\pm$ .06	0.16 $\pm$ .07	0.14 $\pm$ 0.12
Sn	0.22 $\pm$ 0.08	0.96 $\pm$ 0.30	0.60 $\pm$ .15	0.36 $\pm$ .10	0.53 $\pm$ 0.32
Sb	1.39 $\pm$ 0.34	4.1 $\pm$ 0.9	1.31 $\pm$ 0.30	5.8 $\pm$ .09	3.1 $\pm$ 2.2
Te	0.12 $\pm$ 0.04	< 0.06	0.06 $\pm$ 0.03	0.08 $\pm$ .06	0.072 $\pm$ 0.038
Hg	< 0.13	< 0.4	< 0.2	< 0.2	< 0.2
Pb	17.8 $\pm$ .9	21.5 $\pm$ 2.6	46 $\pm$ 3	27.5 $\pm$ 1.5	28 $\pm$ 13
Bi	2.4 $\pm$ 0.1	0.6 $\pm$ 0.2	0.6 $\pm$ 0.1	0.5 $\pm$ 0.1	1.0 $\pm$ 0.92
Mass ( $\mu\text{g}$ )	2121	93	3774	8468	
F/C	910	6.8	56	47	254 $\pm$ 437

Table 12

Percent Elemental Composition of Emission from Reverbatory Furnace  
Slag Skim: Fine Fraction ( < 2.5  $\mu$ m)

Element	Sample Identification				
	MF893	MF863	MF867	MF871	Mean $\pm$ SD
Al	< 0.2	< 0.2	< 0.2	< 0.2	< 0.2
Si	< 0.2	< 0.2	< 0.2	< 0.2	< 0.2
S	< 0.8	< 1.0	< 1.0	< 1.0	< 1.0
Cl	< 0.2	< 0.2	< 0.2	< 0.2	< 0.2
K	< 0.5	< 0.5	< 0.5	< 0.5	< 0.5
Ca	< 0.5	< 0.5	< 0.5	< 0.5	< 0.5
Ti	< 0.02	< 0.03	< 0.02	< 0.03	< 0.3
V	< 0.01	< 0.01	< 0.01	< 0.01	< 0.01
Cr	< 0.01	< 0.01	< 0.01	< 0.01	< 0.01
Mn	< 0.01	< 0.01	< 0.01	< 0.01	< 0.01
Fe	0.21 $\pm$ .02	0.17 $\pm$ .01	0.19 $\pm$ .02	0.19 $\pm$ .02	0.19 $\pm$ 0.016
Ni	< 0.03	< 0.03	< 0.03	< 0.03	< 0.03
Cu	0.15 $\pm$ .02	0.15 $\pm$ .02	0.15 $\pm$ .01	0.16 $\pm$ .02	0.15 $\pm$ 0.0050
Zn	1.8 $\pm$ .1	1.7 $\pm$ .1	1.7 $\pm$ .1	1.7 $\pm$ .1	1.7 $\pm$ 0.050
As	55 $\pm$ 4	62 $\pm$ 5	60 $\pm$ 5	63 $\pm$ 5	60 $\pm$ 3.6
Se	< 0.2	< 0.2	< 0.2	< 0.2	< 0.2
Br	< 0.2	< 0.2	< 0.2	< 0.2	< 0.2
Rb	< 0.1	< 0.1	< 0.1	< 0.1	< 0.1
Sr	< 0.1	< 0.1	< 0.1	< 0.1	< 0.1
Y	< 0.1	< 0.1	< 0.1	< 0.1	< 0.1
Mo	0.09 $\pm$ .01	0.09 $\pm$ .01	0.10 $\pm$ .01	0.09 $\pm$ .01	0.092 $\pm$ 0.0050
Ag	0.010 $\pm$ .003	0.012 $\pm$ .003	0.010 $\pm$ .003	0.013 $\pm$ .003	0.011 $\pm$ 0.0015
Cd	0.61 $\pm$ .07	0.69 $\pm$ .08	0.77 $\pm$ .09	0.76 $\pm$ .06	0.63 $\pm$ 0.22
In	0.013 $\pm$ .003	0.012 $\pm$ .003	0.011 $\pm$ .003	0.013 $\pm$ .003	0.012 $\pm$ 0.00096
Sn	0.15 $\pm$ .04	0.14 $\pm$ .03	0.11 $\pm$ .03	0.11 $\pm$ .03	0.13 $\pm$ 0.021
Sb	1.11 $\pm$ .15	1.06 $\pm$ .14	1.07 $\pm$ .12	1.04 $\pm$ .11	1.1 $\pm$ 0.029
Te	0.071 $\pm$ .017	0.092 $\pm$ .15	0.12 $\pm$ .02	0.076 $\pm$ .015	0.090 $\pm$ 0.022
Hg	< 0.3	< 0.3	< 0.3	< 0.3	< 0.3
Pb	5.2 $\pm$ .3	6.8 $\pm$ .4	5.4 $\pm$ .3	6.5 $\pm$ 0.4	6.0 $\pm$ 0.79
Bi	0.26 $\pm$ 0.05	0.50 $\pm$ .08	0.32 $\pm$ .05	0.39 $\pm$ .05	0.37 $\pm$ 0.10
Mass ( $\mu$ g)	21,779	9242	13,733	10,044	--
F/C	25	30	25	27	26.8



Table 13

Percent Elemental Composition of Emissions from Number 1  
Brick Flue: Coarse Fraction ( $> 2.5 \mu\text{m}$ )<sup>a</sup>

Element	Sample Identification				
	MC876	MC878	MC880	MC884	Mean $\pm$ SD
Al	< 2	< 2	< 2	< 2	< 2
Si	< 1	< 1	< 1	< 1	< 1
S	< 2	< 2	< 2	< 2	< 2
Cl	< 0.5	< 0.5	< 0.5	< 0.5	< 0.5
K	< 0.5	< 0.5	< 0.5	< 0.5	< 0.5
Ca	< 2	< 2	< 2	< 2	< 2
Ti	< 0.2	< 0.2	< 0.2	< 0.2	< 0.2
V	0.016 $\pm$ .005	0.010 $\pm$ .007	0.018 $\pm$ .06	0.015 $\pm$ .005	0.015 $\pm$ 0.003
Cr	0.021 $\pm$ .005	0.020 $\pm$ .005	0.011 $\pm$ .06	0.015 $\pm$ .005	0.017 $\pm$ 0.005
Mn	0.011 $\pm$ .005	0.013 $\pm$ .005	0.018 $\pm$ .05	0.016 $\pm$ .006	0.015 $\pm$ 0.003
Fe	0.34 $\pm$ .05	0.48 $\pm$ .06	0.40 $\pm$ .06	0.37 $\pm$ .04	0.40 $\pm$ 0.06
Ni	0.06 $\pm$ .02	0.10 $\pm$ .02	0.06 $\pm$ .02	0.07 $\pm$ .01	0.07 $\pm$ 0.02
Cu	2.1 $\pm$ 0.2	2.3 $\pm$ .3	2.6 $\pm$ .3	2.6 $\pm$ .3	2.4 $\pm$ 0.2
Zn	2.3 $\pm$ 0.3	5.0 $\pm$ .7	5.2 $\pm$ .7	3.5 $\pm$ .4	4.0 $\pm$ 1.4
As	46 $\pm$ 5	37 $\pm$ 4	42 $\pm$ 5	25 $\pm$ 4	38 $\pm$ 9
Se	< 0.2	< 0.2	< 0.2	< 0.2	< 0.2
Br	< 1.0	< 1.0	< 1.0	< 1.0	< 1.0
Rb	< 0.1	< 0.1	< 0.1	< 0.1	< 0.1
Sr	< 0.1	< 0.1	< 0.1	< 0.1	< 0.1
Y	< 0.1	< 0.1	< 0.1	< 0.1	< 0.1
Mo	0.116 $\pm$ .014	0.185 $\pm$ .033	0.122 $\pm$ .029	0.111 $\pm$ .017	0.134 $\pm$ 0.035
Ag*	0.10 $\pm$ .03	0.10 $\pm$ .03	0.19 $\pm$ .03	0.09 $\pm$ .03	0.12 $\pm$ 0.05
Cd*	0.58 $\pm$ .11	0.40 $\pm$ .10	0.41 $\pm$ .10	0.44 $\pm$ .10	0.46 $\pm$ 0.08
In*	0.02 $\pm$ .01	< 0.02	< 0.02	< 0.02	< 0.02
Sn*	0.31 $\pm$ .05	0.37 $\pm$ .05	0.48 $\pm$ .07	0.38 $\pm$ .05	0.39 $\pm$ 0.07
Sb*	5.3 $\pm$ .4	5.7 $\pm$ .4	6.1 $\pm$ .5	5.2 $\pm$ .5	5.6 $\pm$ 0.4
Te*	0.20 $\pm$ .06	0.14 $\pm$ .06	0.21 $\pm$ .07	0.18 $\pm$ .06	0.18 $\pm$ 0.03
Hg	< 0.5	< 0.5	< 0.5	< 0.5	< 0.5
Pb	12.6 $\pm$ 1.6	16 $\pm$ 2	17 $\pm$ 2	17 $\pm$ 2	16 $\pm$ 2
Bi	-	-	-	-	-
Mass ( $\mu\text{g}$ ) <sup>a</sup>	1142	674	768	832	-
F/C	5.5	8.4	8.1	7.6	7.2 <sup>b</sup>

<sup>a</sup>Based on mass and elemental composition after subtracting fine particles mass deposited with coarse particles.

\*Fine fraction not subtracted.

<sup>b</sup>All values included in average.

Table 14

Percent Elemental Composition of Emissions from the Number 4  
Converter Secondary Hood: Coarse Fraction ( > 2.5  $\mu\text{m}$ )<sup>a</sup>

Element	Sample Identification	
	MC896	MC872
Al	< 3	-
Si	< 10	-
S	< 30	-
Cl	< 5	-
K	< 5	-
Ca	< 2	-
Ti	< 0.2	-
V	< 0.05	-
Cr	< 0.05	-
Mn	-	-
Fe	7.1 $\pm$ 1.2	-
Ni	-	-
Cu	9.4 $\pm$ 1.5	-
Zn	< 2	-
As	< 22	-
Se	< 0.4	-
Br	< 1.0	-
Rb	< 0.3	-
Sr	< 0.2	-
Y	< 2.0	-
Mo	< 0.2	-
Ag*	0.16 $\pm$ .04	0.38 $\pm$ 0.09
Cd*	0.26 $\pm$ .05	0.17 $\pm$ 0.09
In*	< 0.05	< 0.05
Sn*	0.42 $\pm$ .08	< 0.05
Sb*	1.73 $\pm$ .3	1.74 $\pm$ .3
Te*	< 0.02	0.4 $\pm$ 0.1
Hg	< 0	-
Pb	< 20	-
Bi	-	-
Mass ( $\mu\text{g}$ ) <sup>a</sup>	68	13.7
F/C	56	6.8

<sup>a</sup>Net deposit after subtracting fine particles deposited with coarse fraction.

\*Fine fraction not subtracted.

Table 15

Percent Elemental Composition of Emissions from Reverbatory  
Furnace Slag Skim: Coarse Fraction ( > 2.5  $\mu\text{m}$ )

Element	Sample Identification		
	MC864	MC870	Mean $\pm$ SD
Al	< 1.0	< 1.0	< 1.0
Si	< 1.0	< 1.0	< 1.0
S	< 5	< 5	< 5
Cl	< 0.5	< 0.5	< 0.5
K	< 2	< 2	< 2
Ca	< 0.8	< 0.8	< 0.8
Ti	< 0.06	< 0.06	< 0.06
V	< 0.02	< 0.02	< 0.02
Cr	< 0.01	< 0.01	< 0.01
Mn	< 0.02	< 0.03	< 0.03
Fe	0.34 $\pm$ .06	0.42 $\pm$ .07	0.38 $\pm$ 0.06
Ni	< 0.05	< 0.05	< 0.05
Cu	0.175 $\pm$ .05	0.158 $\pm$ .04	0.167 $\pm$ 0.01
Zn	0.88 $\pm$ 0.45	0.75 $\pm$ .39	0.82 $\pm$ 0.09
As	69 $\pm$ 18	72 $\pm$ 16	71 $\pm$ 2
Se	< 0.3	< 0.3	< 0.3
Br	< 0.9	< 0.9	< 0.9
Rb	< 0.3	< 0.3	< 0.3
Sr	< 0.05	< 0.05	< 0.05
Y	< 0.2	< 0.2	< 0.2
Mo	0.10 $\pm$ .04	0.115 $\pm$ .03	0.11 $\pm$ 0.01
Ag	< 0.03	< 0.03	< 0.03
Cd	0.85 $\pm$ .19	0.20 $\pm$ .08	0.53 $\pm$ 0.46
In	0.023 $\pm$ .015	< 0.02	< 0.02
Sn	0.19 $\pm$ .08	0.22 $\pm$ 0.10	0.21 $\pm$ 0.02
Sb	0.92 $\pm$ .15	1.04 $\pm$ 0.18	0.98 $\pm$ 0.08
Te	0.14 $\pm$ .07	0.12 $\pm$ 0.08	0.13 $\pm$ 0.01
Hg	< 0.5	< 0.5	< 0.5
Pb	8.2 $\pm$ 2.0	7.7 $\pm$ 1.9	8.0 $\pm$ 0.4
Bi	-	-	-
Mass ( $\mu\text{g}$ )	303	374	
F/C	30	27	

Table 16

## Comparison of Elemental Composition of Slag

	<u>This Study</u> <u>Coarse Fraction</u>	<u>Reference No. 7</u> <sup>(a)</sup>
Al	1.8 ± 0.2	2.2
Si	14.1 ± 0.9	13.
Ca	3.6 ± 0.2	3.9
Ti	0.30 ± 0.05	0.17
V	0.04 ± 0.01	0.004
Cr	0.11 ± 0.02	0.068
Mn	0.13 ± 0.02	0.15
Fe	21.6 ± 1.4	42. (oxide?)
Ni	0.041 ± .005	0.008
Cu	1.96 ± 0.10	0.098
Zn	1.74 ± 0.09	1.3
As	1.88 ± 0.12	1.12 <sup>(b)</sup>
Sr	0.019 ± 0.004	0.17
Mo	0.100 ± 0.015	0.096
Ag	< 0.02	0.0006
Cd	0.05 ± 0.01	< 0.03
Sn	< 0.06	0.038
Sb	0.19 ± 0.03	0.35
Hg	< 0.03	< 0.09
Pb	0.89 ± 0.08	0.18

(a) Semiquantitative spectrographic analysis

(b) Atomic absorption analysis

Table 17

Elemental Concentration of Ambient Samples ( $\mu\text{g}/\text{m}^3$ )\*

Element	Sample No.									
	181714	131322	131369	131382	131310	181753	182120	182488	182256	182495
Fe	1.2 $\pm$ .2	1.9 $\pm$ .2	1.7 $\pm$ .2	1.9 $\pm$ .2	0.93 $\pm$ .15	1.2 $\pm$ .2	0.96 $\pm$ .10	0.64 $\pm$ .09	2.6 $\pm$ .5	0.66 $\pm$ .09
Cu	1.25 $\pm$ .15	2.1 $\pm$ .2	0.32 $\pm$ .03	1.1 $\pm$ .1	0.51 $\pm$ .06	2.2 $\pm$ .2	0.48 $\pm$ .05	0.21 $\pm$ .03	2.6 $\pm$ 0.2	0.22 $\pm$ .03
As	2.5 $\pm$ .3	2.4 $\pm$ .3	0.20 $\pm$ .05	0.51 $\pm$ .08	0.34 $\pm$ .06	2.9 $\pm$ .3	1.6 $\pm$ .2	0.21 $\pm$ .04	2.8 $\pm$ .3	0.21 $\pm$ .04
Se	0.039 $\pm$ .008	0.04 $\pm$ .01	< .005	< .005	< .005	0.023 $\pm$ .006	0.029 $\pm$ .006	< .005	0.08 $\pm$ .02	< .005
Br	-	-	0.12 $\pm$ .06	-	-	-	-	-	-	-
Ag	0.02 $\pm$ 0.01	0.016 $\pm$ .008	< .03	< .03	< .03	0.04 $\pm$ .02	< .03	< .03	0.02 $\pm$ .01	< .03
Cd	< 0.03	< 0.03	< .03	< .03	< .03	0.03 $\pm$ .02	< .03	< .03	< .01	< .03
In	< 0.03	< .03	< .03	< .03	<	<	<	<	<	< .03
Sn	< 0.03	0.11 $\pm$ .03	< .03	< .03	< .02	0.08 $\pm$ .03	< .03	< .03	0.03 $\pm$ .01	< .03
Sb	0.12 $\pm$ 0.06	0.12 $\pm$ .04	0.06 $\pm$ .04	< .03	0.06 $\pm$ .04	0.20 $\pm$ .06	0.07 $\pm$ .04	< .04	0.16 $\pm$ .03	< .04
Te	< .06	< .05	-	-	-	-	-	-	< .03	-
Hg	0.015 $\pm$ .010	0.02 $\pm$ .01	< .01	< .01	< 0.01	0.03 $\pm$ .01	< .01	< .01	0.025 $\pm$ .010	< .01
Pb	0.70 $\pm$ .08	1.65 $\pm$ .15	0.53 $\pm$ .05	0.95 $\pm$ .09	0.16 $\pm$ .02	1.36 $\pm$ .15	0.63 $\pm$ .08	0.31 $\pm$ .04	1.62 $\pm$ 0.15	0.29 $\pm$ .03
Site	P14	P14	P14	P14	P15	P14	P15	P2	P14	P15
Date	9/18/83	1/13/84	1/18/84	1/19/84	1/13/84	9/21/83	11/8/83	12/20/83	12/20/83	12/20/83

\*S, Cl, K, Ca, Ti, V, Cr, Mn, Ni, Zn, Ga, Rb, Sr, Y, Zr, Mo, Pd, Ba, and La were also measured, but the results were not substantially different from the blank or there were substantial potential interferences from the glass fiber impurities.

Table 18a

Correlation Matrix  
(10 Ambient glass fiber filters)

Element	Fe	Cu	As	Sb
Cu	0.71			
As	0.45	0.88		
Sb	0.40	0.86	0.92	
Pb	0.77	0.95	0.81	0.75

Table 18b

Slope Matrix  
(10 Ambient glass fiber filters)

Element	Fe	Cu	As	Sb
Cu	0.50			
As	0.24	0.67		
Sb	4.39	13.60	18.99	
Pb	0.89	1.55	1.73	0.078

Table 18c

Intercept Matrix  
(10 Ambient glass fiber filters)

Element	Fe	Cu	As	Sb
Cu	0.82			
As	1.04	0.18		
Sb	0.97	-0.12	-0.34	
Pb	0.64	-0.17	-0.053	0.026

Table 19

CMDED RESULTS FOR CMB # MB338

TOTAL SIZE FRACTION

SITE: P14

SAMPLING DATE: 83 918 SITE CODE: 6

SAMPLING DURATION: 24 HRS. WITH START HOUR: 0

EFFECTIVE VARIANCE FITTING. REDUCED CHI SQUARE: 32.185 D OF F: 3

-----(SOURCE)-----		-----(UG/M3)-----		-----(PERCENT)-----	
1	SLGSKM *	2.902+-	.649	6.749+-	1.546
2	BRKFLU *	2.994+-	.534	6.962+-	1.288
-----					
TOTAL:		5.895+-	.841	13.710+-	2.067
-----					
--(SPECIE)---		--(MEAS. UG/M3)---		--(%)---	
1	Fe *	1.200+-	.200	2.791	.014+- .001
2	Cu *	1.250+-	.150	2.907	.094+- .008
3	As *	2.500+-	.300	5.814	.246+- .130
4	Sb *	.120+-	.060	.279	.212+- .017
5	Pb *	.700+-	.080	1.628	.713+- .036

MEAS. AMB. MASS (UG/M3): 43.0

\* - FITTING SOURCE OR ELEMENT

Table 20

CMDED RESULTS FOR CMB # MB338

TOTAL SIZE FRACTION

SITE: P14

SAMPLING DATE: 83 918 SITE CODE: 6

SAMPLING DURATION: 24 HRS. WITH START HOUR: 0

EFFECTIVE VARIANCE FITTING. REDUCED CHI SQUARE: .064 D OF F: 2

-----(SOURCE)-----		-----(UG/M3)-----		-----(PERCENT)-----	
1	SLGSKM *	3.337+-	.646	7.760+-	1.550
2	BRKFLU *	1.126+-	.563	2.618+-	1.315
7	RDBLDG *	9.564+-	1.045	22.243+-	2.661
-----					
TOTAL:		14.027+-	1.351	32.620+-	3.523
-----					
--(SPECIE)---		--(MEAS. UG/M3)---		--(%)---	
1	Fe *	1.200+-	.200	2.791	1.138+- .057
2	Cu *	1.250+-	.150	2.907	1.282+- .067
3	As *	2.500+-	.300	5.814	2.502+- .125
4	Sb *	.120+-	.060	.279	.119+- .008
5	Pb *	.700+-	.080	1.628	.699+- .034

MEAS. AMB. MASS (UG/M3): 43.0

\* - FITTING SOURCE OR ELEMENT

Table 21

CMRDED RESULTS FOR CMR # MB338

TOTAL SIZE FRACTION

SITE: F14

SAMPLING DATE: 83 918 SITE CODE: 6

SAMPLING DURATION: 24 HRS. WITH START HOUR: 0

EFFECTIVE VARIANCE FITTING. REDUCED CHI SQUARE: .055 D OF F: 2

----(SOURCE)-----		(UG/M3)		(PERCENT)	
3	HOOD *	1.788+-	.886	4.158+-	2.070
6	RDFQB *	5.961+-	.712	13.862+-	1.789
14	ASPLNT *	3.715+-	.894	8.639+-	2.122
TOTAL: *		11.464+-	1.446	26.660+-	3.606

-(SPECIE)---		(MEAS. UG/M3)---		(%)---		(CALC. UG/M3)---		(RATIO)-----	
1	Fe *	1.200+-	.200	2.791	1.171+-	.054	.976+-	.169	Fe
2	Cu *	1.250+-	.150	2.907	1.268+-	.063	1.014+-	.132	Cu
3	As *	2.500+-	.300	5.814	2.478+-	.226	.991+-	.149	As
4	Sb *	.120+-	.080	.279	.139+-	.040	1.158+-	.667	Sb
5	Pb *	.700+-	.080	1.628	.682+-	.233	.975+-	.350	Pb

MEAS. AMB. MASS (UG/M3): 43.0

\* - FITTING SOURCE OR ELEMENT



CMRDEQ RESULTS FOR CMR # MB335

TOTAL SIZE FRACTION

SITE: P14

SAMPLING DATE: 83 918 SITE CODE: 6

SAMPLING DURATION: 24 HRS. WITH START HOUR: 0

EFFECTIVE VARIANCE FITTING. REDUCED CHI SQUARE: 1.941 D OF F: 1

	(SOURCE)		(UG/M3)		(PERCENT)
2	BRKFLU *	3.209+-	.030	6.067+-	1.163
6	RDFOB *	5.991+-	.285	13.700+-	1.770
14	ASPLNT *	3.366+-	.08	7.594+-	1.682
TOTAL:		11	27.561+-	1.891	

	(SPECIE)	(MEAS. MASS)	(CALC. UG/M3)	(RATIO)	
1	Fe *	1.200+-	.299	1.149+-	.053
2	Cu *	1.200+-	.100	1.297+-	.060
3	As *	2.400+-	.300	2.409+-	.119
4	Sb *	1.100+-	.060	.230+-	.016
5	Pb *	1.700+-	.080	1.628	.641+-

MEAS. AMB. MASS (UG/M3): 43.0

\* - FITTING SOURCE OR ELEMENT

Table 23

CMRDEQ RESULTS FOR CMR # MB335

TOTAL SIZE FRACTION

SITE: P14

SAMPLING DATE: 84 113 SITE CODE: 6

SAMPLING DURATION: 24 HRS. WITH START HOUR: 0

EFFECTIVE VARIANCE FITTING. REDUCED CHI SQUARE: .002 D OF F: 1

	(SOURCE)		(UG/M3)		(PERCENT)
1	BLSSKM *	1.981+-	.646	3.962+-	1.307
2	BRKFLU *	.884+-	.277	1.769+-	1.549
7	RDBLDG *	15.924+-	1.295	31.848+-	3.037
13	COTTRL *	2.773+-	.24	4.758+-	1.270
TOTAL:		21.563+-	1.462	4.758+-	4.097

	(SPECIE)	(MEAS. MASS)	(CALC. UG/M3)	(RATIO)	
1	Fe *	1.200+-	.299	1.893+-	.096
2	Cu *	2.000+-	.200	2.107+-	.112
3	As *	2.400+-	.300	2.400+-	.108
4	Sb *	1.100+-	.060	.120+-	.010
5	Pb *	1.650+-	.150	3.300	1.650+-

MEAS. AMB. MASS (UG/M3): 50.0

\* - FITTING SOURCE OR ELEMENT

Table 24

CMBDEQ RESULTS FOR CMB # MB335

TOTAL SIZE FRACTION

SITE: P14

SAMPLING DATE: 84 113 SITE CODE: 6

SAMPLING DURATION: 24 HRS. WITH START HOUR: 0

EFFECTIVE VARIANCE FITTING. REDUCED CHI SQUARE: .072 D OF F: 1

-----(SOURCE)-----		-----(UG/M3)-----		-----(PERCENT)-----	
1	SLGSKM *	1.863+-	.655	3.726+-	1.324
2	BRKFLU *	1.091+-	.763	2.182+-	1.531
6	RDFOB *	10.768+-	.871	21.536+-	2.049
13	COTTRL *	3.097+-	.636	6.193+-	1.310
TOTAL:		16.819+-	1.475	33.637+-	3.396

--(SPECIE)---		---(MEAS. UG/M3)---		---(%)---		---(CALC. UG/M3)---		---(RATIO)---	
1	Fe *	1.900+-	.200	3.800	1.943+-	.097	1.023+-	.119	Fe
2	Cu *	2.100+-	.200	4.200	2.058+-	.108	.980+-	.107	Cu
3	As *	2.400+-	.300	4.800	2.399+-	.119	1.000+-	.134	As
4	Sb *	.120+-	.040	.240	.121+-	.007	1.007+-	.341	Sb
5	Pb *	1.650+-	.150	3.300	1.650+-	.095	1.000+-	.106	Pb

MEAS. AMB. MASS (UG/M3): 50.0

\* - FITTING SOURCE OR ELEMENT

Table 25

CMBDEQ RESULTS FOR CMB # MB336

TOTAL SIZE FRACTION

SITE: P14

SAMPLING DATE: 84 118 SITE CODE: 6

SAMPLING DURATION: 24 HRS. WITH START HOUR: 0

EFFECTIVE VARIANCE FITTING. REDUCED CHI SQUARE: 2.967 D OF F: 2

-----(SOURCE)-----		-----(UG/M3)-----		-----(PERCENT)-----	
3	HOOD *	.817+-	.289	.717+-	.256
4	SLGDMF *	6.959+-	1.128	6.105+-	1.035
7	RDBLDG *	1.352+-	.327	1.186+-	.293
TOTAL:		9.129+-	1.209	8.008+-	1.134

--(SPECIE)---		---(MEAS. UG/M3)---		---(%)---		---(CALC. UG/M3)---		---(RATIO)---	
1	Fe *	1.700+-	.200	1.491	1.665+-	.098	.979+-	.129	Fe
2	Cu *	.320+-	.030	.281	.321+-	.015	1.004+-	.105	Cu
3	As *	.200+-	.050	.175	.376+-	.090	1.879+-	.652	As
4	Sb *	.060+-	.040	.053	.041+-	.018	.677+-	.543	Sb
5	Pb *	.530+-	.050	.465	.333+-	.106	.628+-	.209	Pb

MEAS. AMB. MASS (UG/M3): 114.0

\* - FITTING SOURCE OR ELEMENT

Table 26

CMBDEQ RESULTS FOR CMB # MB337

TOTAL SIZE FRACTION

SITE: P14

SAMPLING DATE: 84 119 SITE CODE: 6

SAMPLING DURATION: 24 HRS. WITH START HOUR: 0

EFFECTIVE VARIANCE FITTING. REDUCED CHI SQUARE: 2.475 D OF F: 2

----(SOURCE)-----		----(UG/M3)-----		----(PERCENT)-----	
4	SLGDMP *	3.980+-	1.207	2.823+-	.867
6	RDFOB *	5.471+-	.677	3.880+-	.517
13	COTTRL *	1.841+-	.231	1.306+-	.176
TOTAL:		11.293+-	1.403	8.009+-	1.072

-(SPECIE)----		-(MEAS. UG/M3)----		-(%)----		-(CALC. UG/M3)-----		-(RATIO)-----	
1	Fe *	1.900+-	.200	1.348		1.845+-	.074	.971+-	.109 Fe
2	Cu *	1.100+-	.100	.780		1.107+-	.055	1.006+-	.104 Cu
3	As *	.510+-	.080	.362		.662+-	.056	1.299+-	.231 As
4	Sb *	<	.030	---		.028+-	.002	.000+-	.000 Sb
5	Pb *	.950+-	.090	.674		.816+-	.056	.859+-	.100 Pb

MEAS. AMB. MASS (UG/M3): 141.0

\* - FITTING SOURCE OR ELEMENT

Table 27

CMBDEQ RESULTS FOR CMB # MB337

TOTAL SIZE FRACTION

SITE: P14

SAMPLING DATE: 84 119 SITE CODE: 6

SAMPLING DURATION: 24 HRS. WITH START HOUR: 0

EFFECTIVE VARIANCE FITTING. REDUCED CHI SQUARE: 2.056 D OF F: 2

----(SOURCE)-----		----(UG/M3)-----		----(PERCENT)-----	
3	HOOD *	1.713+-	.548	1.215+-	.393
4	SLGDMP *	4.264+-	1.219	3.024+-	.878
6	RDFOB *	5.366+-	.685	3.806+-	.521
TOTAL:		11.344+-	1.502	8.045+-	1.137

-(SPECIE)----		-(MEAS. UG/M3)----		-(%)----		-(CALC. UG/M3)-----		-(RATIO)-----	
1	Fe *	1.900+-	.200	1.348		1.886+-	.077	.993+-	.112 Fe
2	Cu *	1.100+-	.100	.780		1.106+-	.057	1.005+-	.105 Cu
3	As *	.510+-	.080	.362		.632+-	.189	1.240+-	.418 As
4	Sb *	<	.030	---		.065+-	.038	.000+-	.000 Sb
5	Pb *	.950+-	.090	.674		.615+-	.223	.648+-	.242 Pb

MEAS. AMB. MASS (UG/M3): 141.0

\* - FITTING SOURCE OR ELEMENT

Table 28

CMBDEQ RESULTS FOR CMB # MB334

TOTAL SIZE FRACTION

SITE: P15

SAMPLING DATE: 84 113 SITE CODE: 7

SAMPLING DURATION: 24 HRS. WITH START HOUR: 0

EFFECTIVE VARIANCE FITTING. REDUCED CHI SQUARE: .332 D OF F: 1

---- (SOURCE) -----		(UG/M3) -----		(PERCENT) -----	
2	BRKFLU *	.489+-	.139	1.481+-	.428
4	SLGDMP *	1.685+-	1.431	5.107+-	4.342
8	RD79BT *	4.328+-	4.228	13.116+-	12.829
11	CALCIN *	2.240+-	.462	6.787+-	1.440
TOTAL:		8.742+-	4.490	26.492+-	13.666

-- (SPECIE) ---		(MEAS. UG/M3) ---		--- (%) ---		(CALC. UG/M3) ---		--- (RATIO) ---	
1	Fe *	.930+-	.150	2.818	.929+-	.030	.999+-	.164	Fe
2	Cu *	.510+-	.060	1.545	.509+-	.043	.998+-	.144	Cu
3	As *	.340+-	.060	1.030	.339+-	.020	.996+-	.185	As
4	Sb *	.060+-	.040	.182	.037+-	.003	.621+-	.417	Sb
5	Pb *	.160+-	.020	.485	.162+-	.005	1.013+-	.131	Pb

MEAS. AMB. MASS (UG/M3): 33.0

\* - FITTING SOURCE OR ELEMENT

Table 29

CMBDEQ RESULTS FOR CMB # MB334

TOTAL SIZE FRACTION

SITE: P15

SAMPLING DATE: 84 113 SITE CODE: 7

SAMPLING DURATION: 24 HRS. WITH START HOUR: 0

EFFECTIVE VARIANCE FITTING. REDUCED CHI SQUARE: .677 D OF F: 2

---- (SOURCE) -----		(UG/M3) -----		(PERCENT) -----	
2	BRKFLU *	.571+-	.116	1.731+-	.362
4	SLGDMP *	2.909+-	.813	8.816+-	2.501
11	CALCIN *	2.381+-	.448	7.215+-	1.402
TOTAL:		5.862+-	.936	17.762+-	2.963

-- (SPECIE) ---		(MEAS. UG/M3) ---		--- (%) ---		(CALC. UG/M3) ---		--- (RATIO) ---	
1	Fe *	.930+-	.150	2.818	.940+-	.043	1.010+-	.169	Fe
2	Cu *	.510+-	.060	1.545	.512+-	.045	1.004+-	.148	Cu
3	As *	.340+-	.060	1.030	.280+-	.021	.823+-	.158	As
4	Sb *	.060+-	.040	.182	.042+-	.003	.694+-	.466	Sb
5	Pb *	.160+-	.020	.485	.170+-	.006	1.065+-	.139	Pb

MEAS. AMB. MASS (UG/M3): 33.0

\* - FITTING SOURCE OR ELEMENT

Table 30

EMBEDDED RESULTS FOR CMB # M203

TOTAL SIZE FRACTION

SITE: P14

SAMPLING DATE: 83 921 SITE CODE: 6

SAMPLING DURATION: 24 HRS. WITH START HOUR: 0

EFFECTIVE VARIANCE FITTING. REDUCED CHI SQUARE: 23.151 D OF F: 4

(SOURCE)	(UG/M3)	(PERCENT)
3 GRFLO	16.364+- 4.633	26.394+- 7.500
TOTAL:	16.364+- 4.633	26.394+- 7.500

(SPECIE)	(MEAS. UG/M3)	(%)	(CALC. UG/M3)	(RATIO)
1 Fe *	1.200+- .200	1.935	.043+- .031	.035+- .02
2 Cu *	2.200+- .200	3.548	.180+- .180	.082+- .06
3 As *	2.900+- .300	4.677	4.255+- 1.800	1.467+- .819
4 Sb *	.200+- .060	.323	.507+- .360	2.536+- 1.910
5 Pb *	1.360+- .150	2.194	4.582+- 2.127	3.369+- 1.608

MEAS. AMB. MASS (UG/M3): 62.0

\* - FITTING SOURCE OR ELEMENT

Table 31

EMBEDDED RESULTS FOR CMB # M203

TOTAL SIZE FRACTION

SITE: P14

SAMPLING DATE: 83 921 SITE CODE: 6

SAMPLING DURATION: 24 HRS. WITH START HOUR: 0

EFFECTIVE VARIANCE FITTING. REDUCED CHI SQUARE: 2.812 D OF F: 2

(SOURCE)	(UG/M3)	(PERCENT)
2 GRFLO *	2.886+- .879	4.654+- 1.422
7 REDBUS *	11.582+- 1.292	18.681+- 2.133
10 BLUE *	5.631+- 1.320	9.082+- 2.140
TOTAL:	20.099+- 2.046	32.417+- 3.371

(SPECIE)	(MEAS. UG/M3)	(%)	(CALC. UG/M3)	(RATIO)
1 Fe *	1.200+- .200	1.935	1.538+- .070	1.283+- .11
2 Cu *	2.200+- .200	3.548	1.919+- .083	.540+- .054
3 As *	2.900+- .300	4.677	2.998+- .186	1.034+- .025
4 Sb *	.200+- .060	.323	.255+- .018	1.275+- .393
5 Pb *	1.360+- .150	2.194	1.244+- .039	.915+- .109

MEAS. AMB. MASS (UG/M3): 62.0

\* - FITTING SOURCE OR ELEMENT

Table 32

CMBDEQ RESULTS FOR CMB # MB037

TOTAL SIZE FRACTION

SITE: P15

SAMPLING DATE: 831108 SITE CODE: 7

SAMPLING DURATION: 24 HRS. WITH START HOUR: 0

EFFECTIVE VARIANCE FITTING. REDUCED CHI SQUARE: .131 D OF F: 1

----(SOURCE)-----		(UG/M3)-----		(PERCENT)-----	
4	SLGDMP *	3.224+-	.584	7.008+-	1.318
10	FLUE *	3.317+-	.790	7.211+-	1.755
12	CUCONC *	1.250+-	.431	2.717+-	.947
13	COTTRL *	1.036+-	.302	2.251+-	.665
-----					
TOTAL:		8.826+-	1.115	19.187+-	2.606

-(SPECIE)---		(MEAS. UG/M3)---		(% )----		(CALC. UG/M3)-----		(RATIO)-----	
1	Fe *	.960+-	.100	2.087	.961+-	.046	1.001+-	.115	Fe
2	Cu *	.480+-	.050	1.043	.480+-	.015	1.000+-	.109	Cu
3	As *	1.600+-	.200	3.478	1.611+-	.104	1.007+-	.142	As
4	Sb *	.070+-	.040	.152	.056+-	.003	.795+-	.456	Sb
5	Pb *	.630+-	.080	1.370	.630+-	.033	1.000+-	.137	Pb

MEAS. AMB. MASS (UG/M3): 46.0

\* - FITTING SOURCE OR ELEMENT

Table 33

CMBDEQ RESULTS FOR CMB # MB037

TOTAL SIZE FRACTION

SITE: P15

SAMPLING DATE: 831108 SITE CODE: 7

SAMPLING DURATION: 24 HRS. WITH START HOUR: 0

EFFECTIVE VARIANCE FITTING. REDUCED CHI SQUARE: .107 D OF F: 1

----(SOURCE)-----		(UG/M3)-----		(PERCENT)-----	
3	HOOD *	1.349+-	.817	2.932+-	1.783
4	SLGDMP *	3.241+-	.588	7.046+-	1.326
10	FLUE *	3.038+-	1.134	6.604+-	2.488
12	CUCONC *	1.273+-	.494	2.768+-	1.082
-----					
TOTAL:		8.901+-	1.595	19.350+-	3.600

-(SPECIE)---		(MEAS. UG/M3)---		(% )----		(CALC. UG/M3)-----		(RATIO)-----	
1	Fe *	.960+-	.100	2.087	.960+-	.047	1.000+-	.115	Fe
2	Cu *	.480+-	.050	1.043	.480+-	.021	1.000+-	.113	Cu
3	As *	1.600+-	.200	3.478	1.594+-	.174	.996+-	.165	As
4	Sb *	.070+-	.040	.152	.085+-	.030	1.216+-	.815	Sb
5	Pb *	.630+-	.080	1.370	.607+-	.176	.963+-	.304	Pb

MEAS. AMB. MASS (UG/M3): 46.0

\* - FITTING SOURCE OR ELEMENT

Table 34

CMBDEQ RESULTS FOR CMB # MB029

TOTAL SIZE FRACTION

SITE: F2

SAMPLING DATE: 831220 SITE CODE: 5

SAMPLING DURATION: 24 HRS. WITH START HOUR: 0

EFFECTIVE VARIANCE FITTING. REDUCED CHI SQUARE: .299 D OF F: 2

-----(SOURCE)-----		-----(UG/M3)-----		-----(PERCENT)-----	
4	SLGDMF *	2.221+-	.500	6.346+-	1.461
7	RDBLDG *	1.270+-	.273	3.630+-	.799
13	COTTRL *	.629+-	.101	1.796+-	.300
-----					
TOTAL:		4.120+-	.578	11.771+-	1.748

--(SPECIE)---		---(MEAS. UG/M3)---		---(%)---		-----(CALC. UG/M3)-----		-----(RATIO)-----	
1	Fe *	.840+-	.090	1.829	.632+-	.032	.987+-	.148	Fe
2	Cu *	.210+-	.030	.600	.211+-	.009	1.003+-	.150	Cu
3	As *	.210+-	.040	.600	.236+-	.019	1.122+-	.233	As
4	Sb *	<	.040	---	.012+-	.001	.000+-	.000	Sb
5	Pb *	.310+-	.040	.886	.292+-	.019	.941+-	.136	Pb

MEAS. AMB. MASS (UG/M3): 35.0

\* - FITTING SOURCE OR ELEMENT

Table 35

CMBDEQ RESULTS FOR CMB # MB032

TOTAL SIZE FRACTION

SITE: F14

SAMPLING DATE: 831220 SITE CODE: 6

SAMPLING DURATION: 24 HRS. WITH START HOUR: 0

EFFECTIVE VARIANCE FITTING. REDUCED CHI SQUARE: .075 D OF F: 1

-----(SOURCE)-----		-----(UG/M3)-----		-----(PERCENT)-----	
1	SLGSKM *	2.462+-	.649	4.035+-	1.083
2	BRKFLU *	1.688+-	.603	2.767+-	.997
6	RDFOB *	13.683+-	1.186	22.431+-	2.235
13	COTTRL *	2.485+-	.580	4.074+-	.972
-----					
TOTAL:		20.317+-	1.590	33.307+-	3.078

--(SPECIE)---		---(MEAS. UG/M3)---		---(%)---		-----(CALC. UG/M3)-----		-----(RATIO)-----	
1	Fe *	2.600+-	.500	4.262	2.466+-	.123	.949+-	.188	Fe
2	Cu *	2.600+-	.200	4.262	2.620+-	.137	1.008+-	.094	Cu
3	As *	2.800+-	.300	4.590	2.800+-	.126	1.000+-	.116	As
4	Sb *	.160+-	.030	.262	.160+-	.011	.999+-	.199	Sb
5	Pb *	1.620+-	.150	2.656	1.620+-	.080	1.000+-	.105	Pb

MEAS. AMB. MASS (UG/M3): 61.0

\* - FITTING SOURCE OR ELEMENT

Table 36

CMRDEQ RESULTS FOR CMB # MB038

TOTAL SIZE FRACTION

SITE: P15

SAMPLING DATE: 831220 SITE CODE: 7

SAMPLING DURATION: 24 HRS. WITH START HOUR: 0

EFFECTIVE VARIANCE FITTING. REDUCED CHI SQUARE: .172 D OF F: 2

---- (SOURCE) -----		(UG/M3) -----		(PERCENT) -----	
4	SLGDMP *	2.286+-	.501	5.715+-	1.285
7	RDBLDG *	1.337+-	.274	3.343+-	.705
13	DOTTRL *	.595+-	.085	1.488+-	.226
-----					
TOTAL:		4.218+-	.577	10.546+-	1.537

-- (SPECIE) ---		(MEAS. UG/M3) ---		(%) ---		(CALC. UG/M3) ---		(RATIO) -----	
1	Fe *	.660+-	.090	1.650	.653+-	.033	.990+-	.144	Fe
2	Cu *	.220+-	.030	.550	.220+-	.010	1.002+-	.143	Cu
3	As *	.210+-	.040	.525	.230+-	.018	1.094+-	.226	As
4	Sb *	<	.040	---	.012+-	.001	.000+-	.000	Sb
5	Pb *	.290+-	.030	.725	.282+-	.018	.972+-	.119	Pb

MEAS. AMB. MASS (UG/M3): 40.0

\* - FITTING SOURCE OR ELEMENT



Table 37

## List of Source Code Definitions

	<u>Code</u>	<u>Definition</u>
0001	SLGSKM	Reverbatory Furnace Slag Skim (Fine)
0002	BRKFLU	Number 1 Brick Flue (Fine)
0003	HOOD	Number Converter Secondary Hood (Fine)
0004	SLGDMP	Slag Dump (Coarse)
0005	MARTIN	Martin Mill Weighing Floor (Coarse)
0006	RDFOB	Roadway Dust by Fine Ore Bins (Coarse)
0007	RDBLDG	Roadway Dust by Sample Bldg. (Coarse)
0008	RD79BT	Road Dust 49th and Baltimore (Coarse)
0009	RRTRAK	Railroad Track South Gate (Coarse)
0010	FLUE	No. 1 Flue Dust (Coarse)
0011	CALCIN	Herreshoff Roaster Calcine (Coarse)
0012	CUCONC	Lepanto Copper Concentrate (Coarse)
0013	COTTRL	SO <sub>2</sub> Cottrell Dust (Coarse)
0014	ASPLNT	Arsenic Plant Product (Coarse)

Table 38

## Maximum Source Contributions

Source		181714	131322	181753	182256
Herreschoff	$\mu\text{g}/\text{m}^3$	0.44	0.74	0.77	0.91
Roaster	% As	17.6	30.8	26.6	32.5
Herreschoff	$\mu\text{g}/\text{m}^3$	0.25	0.42	0.44	0.52
Roaster	% As	10.0	17.5	15.2	18.6
Calcine					
Road Dust 49th	$\mu\text{g}/\text{m}^3$	0.47	0.74	0.47	1.0
& Baltimore	% As	18.8	30.8	16.2	35.7
Railroad Track	$\mu\text{g}/\text{m}^3$	1.1	1.8	1.1	2.4
South Gate	% As	44.0	75.0	37.9	85.7
Slag Dump	$\mu\text{g}/\text{m}^3$	0.10	0.17	0.10	0.23
Composite	% As	4.0	7.1	3.4	8.2
Slag Dump	$\mu\text{g}/\text{m}^3$	0.027	0.042	0.027	0.058
Fine Total	% As	1.1	1.8	0.9	2.1
Fine Ore Bin	$\mu\text{g}/\text{m}^3$	0.13	0.21	0.13	0.29
Road Dust	% As	5.2	8.8	4.5	10.4
Sample Bldg.	$\mu\text{g}/\text{m}^3$	0.24	0.39	0.24	0.53
Road Dust	% As	9.6	16.3	8.3	18.9
Martin Mill	$\mu\text{g}/\text{m}^3$	0.47	0.80	0.83	0.99
Floor Dust	% As	18.8	33.3	28.6	35.4
Copper	$\mu\text{g}/\text{m}^3$	0.49	0.83	0.87	1.0
Concentrate	% As	19.6	34.6	30.0	35.7

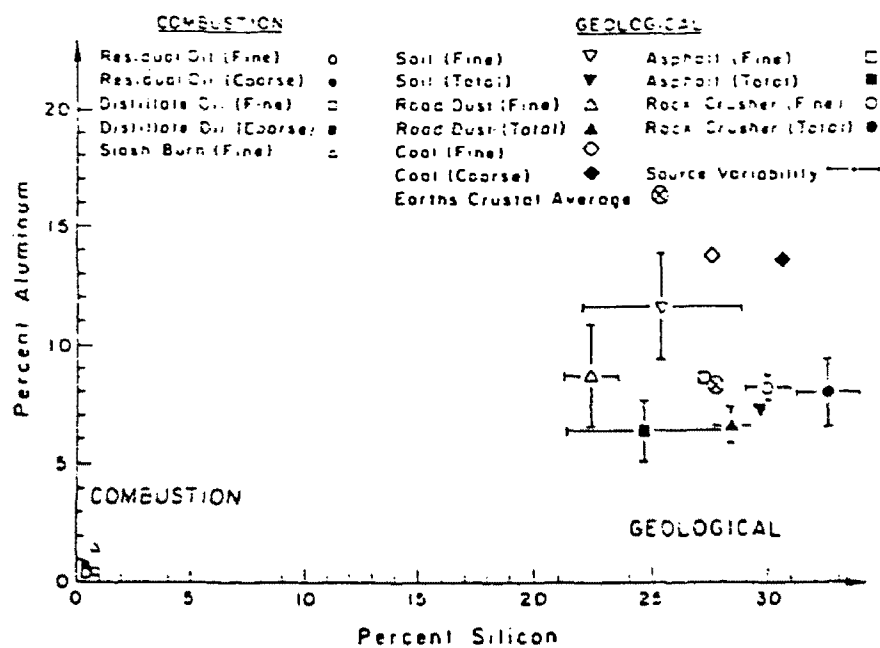


Figure 1. Plot of the percent Al and Si for combustion and geological sources. These sources would be difficult to resolve using only these two elements (dimensions).

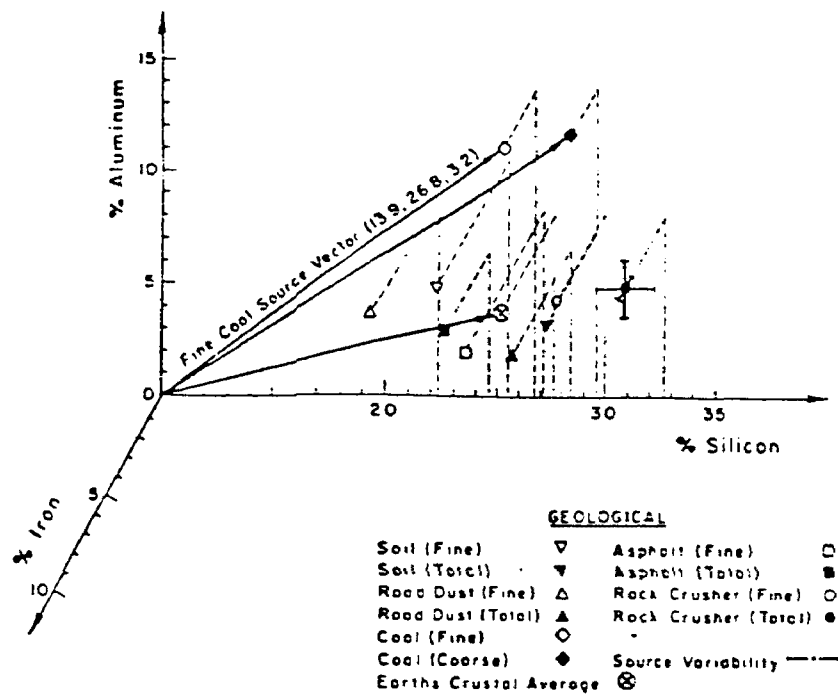


Figure 2. Three dimensional plot of the Fe, Al, and Si in geological type samples. The addition of the Fe dimension effectively improved the source resolving capability, i.e., the angle between the coal fly ash and crustal average has increased.

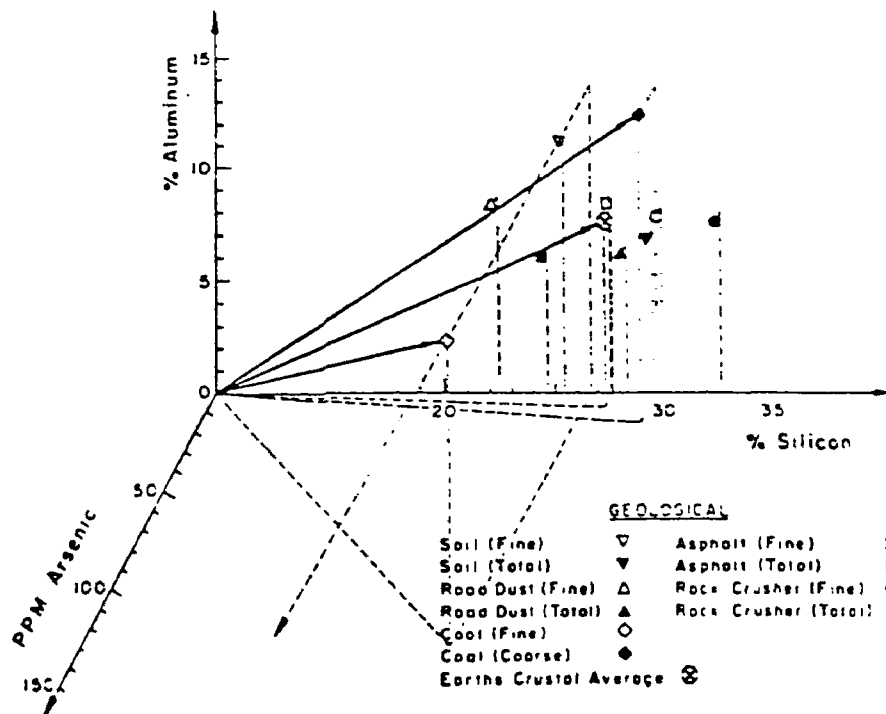


Figure 3. Three dimensional plot for the As, Al, and Si composition in geological samples. The addition of As has greatly improved the separation of the fine coal fly ash from the other sources. Other coal fly ash samples have been reported to contain even higher As concentrations.

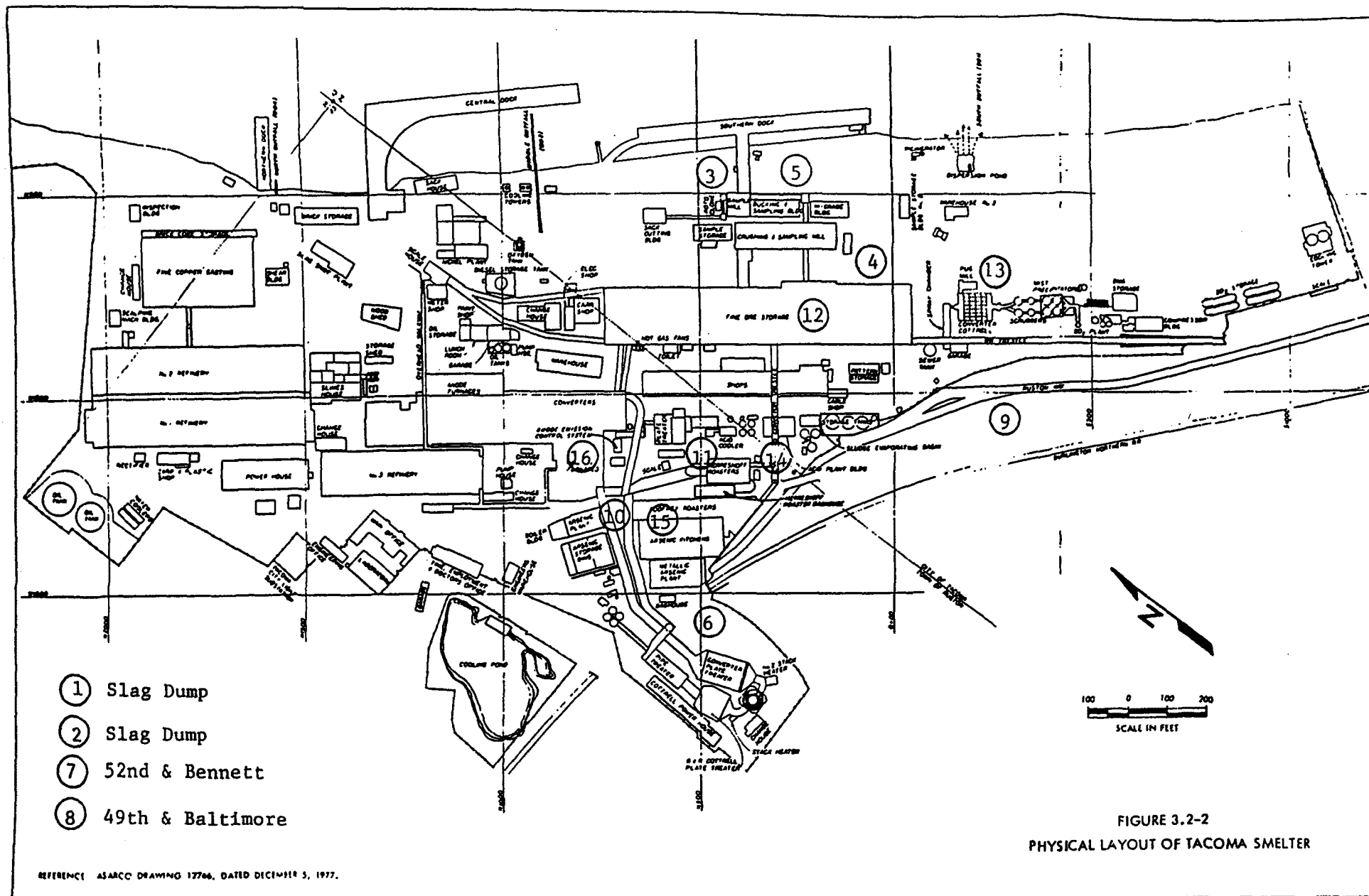


Figure 4. Physical layout of the ASARCO-Tacoma smelter showing the location of the bulk samples collected for analysis.

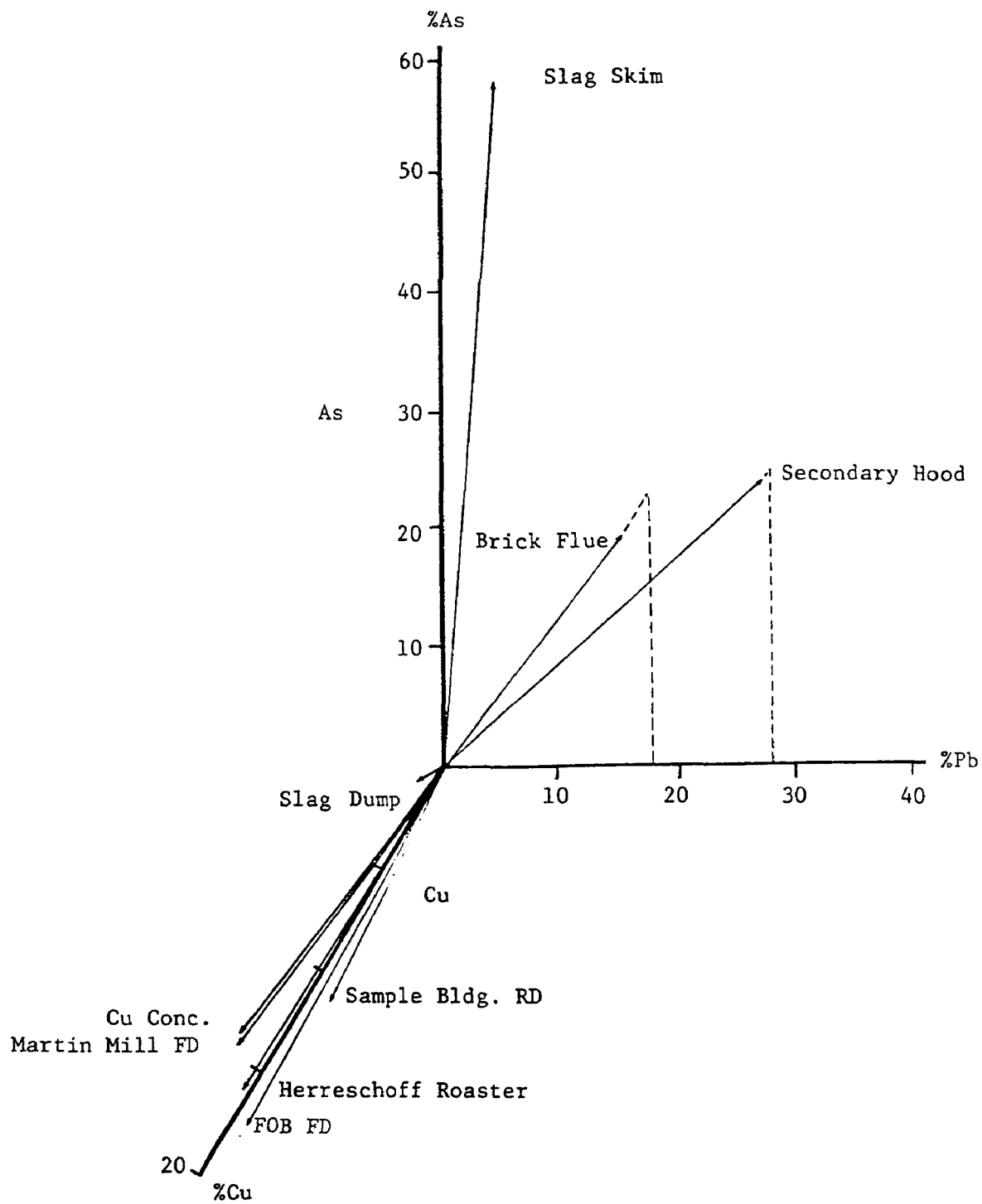


Figure 5. Vectorial representation of three elements from selected source profiles.

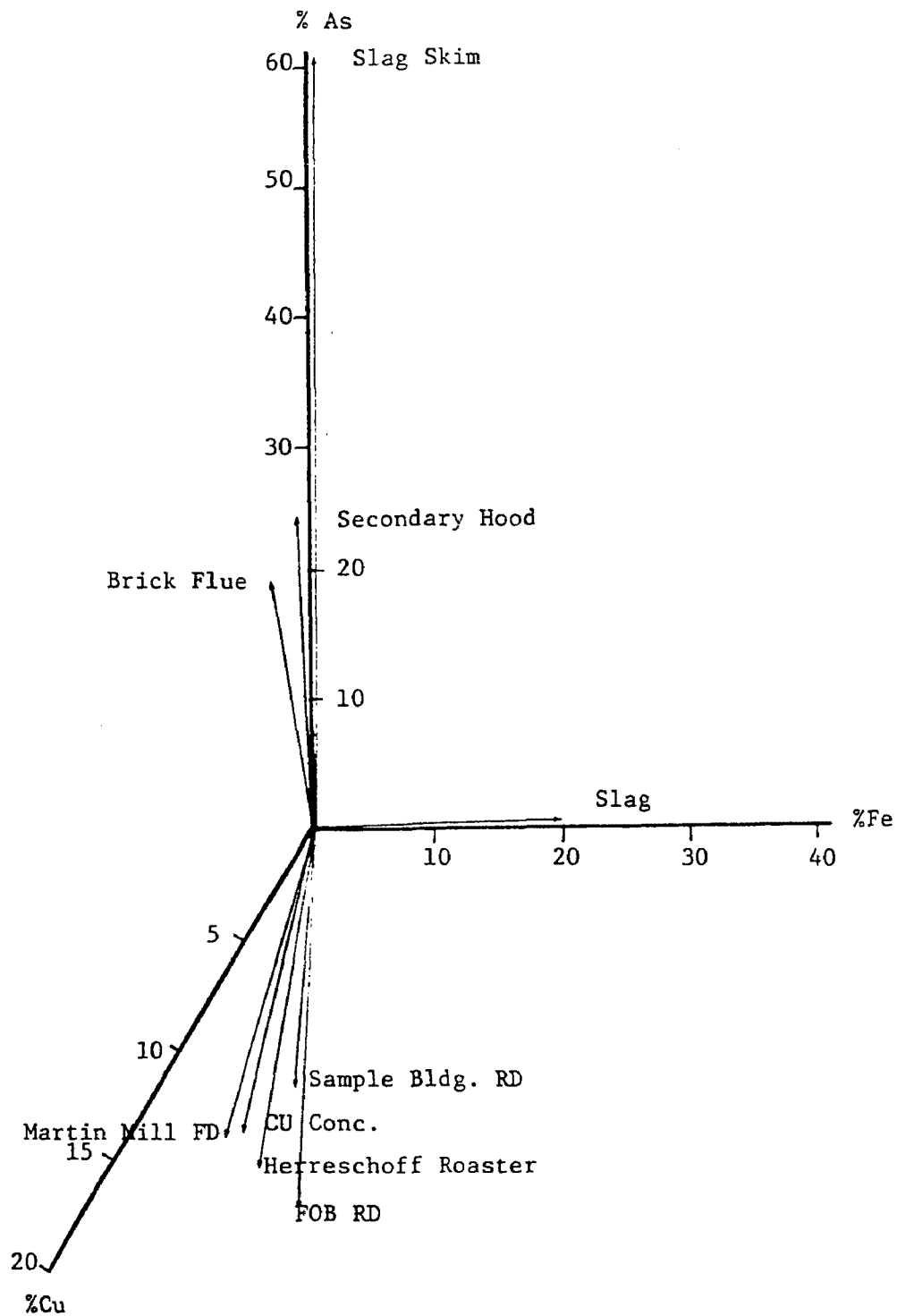


Figure 6. Vectorial representation of three elements from selected source profiles.

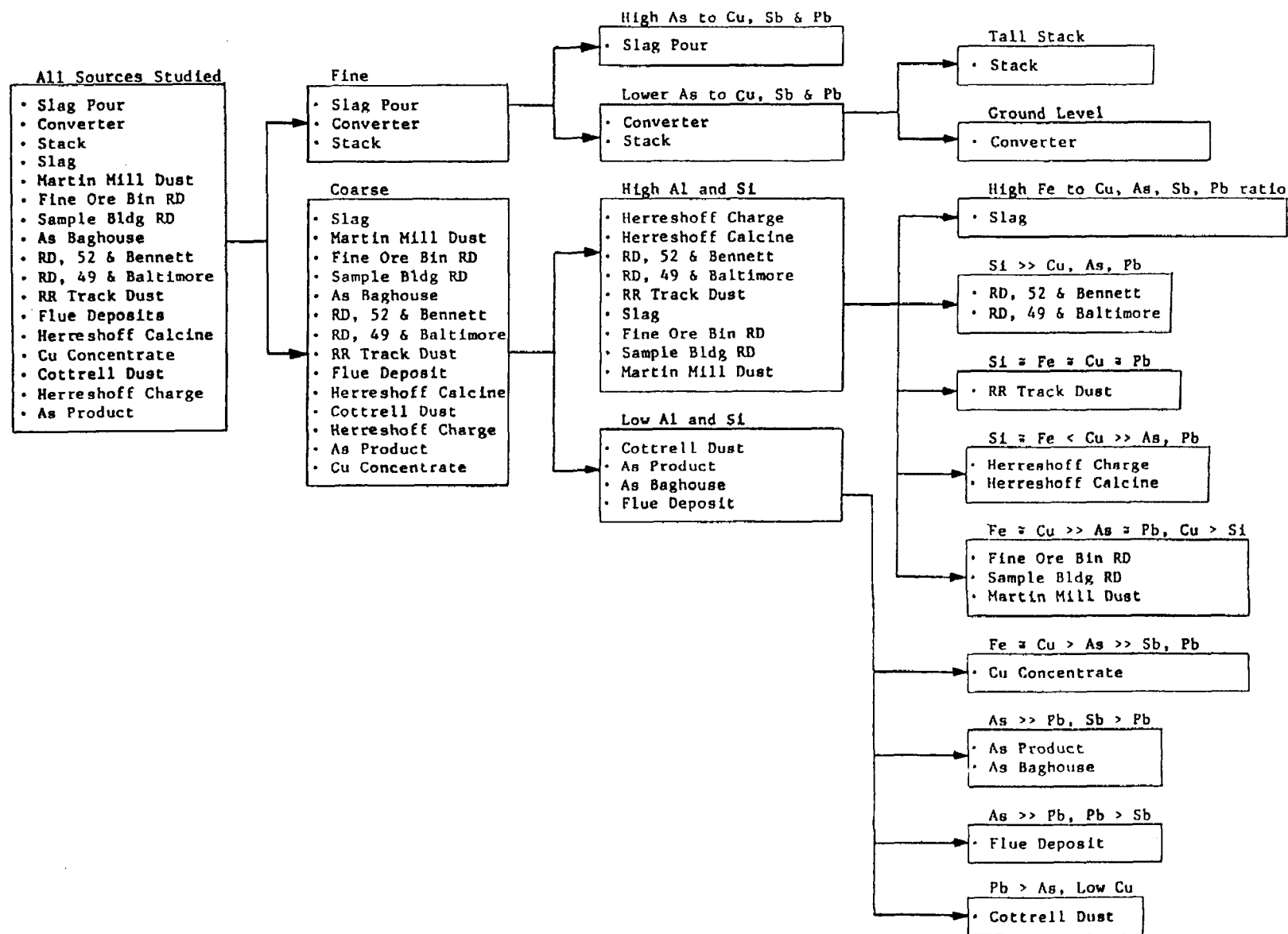


Figure 7. Schematic Categorization of Sources Based on Chemistry and Particle Size



# DIRECT AND INDIRECT CONTRIBUTIONS TO SUSPENDED PARTICULATE MASS

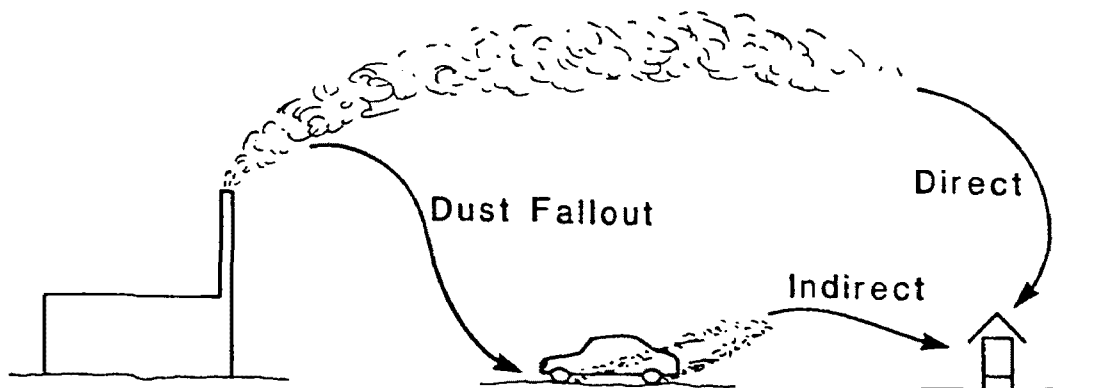


Figure 8. Illustration of direct and indirect smelter impacts on air quality. (From Kellogg report, NEA).

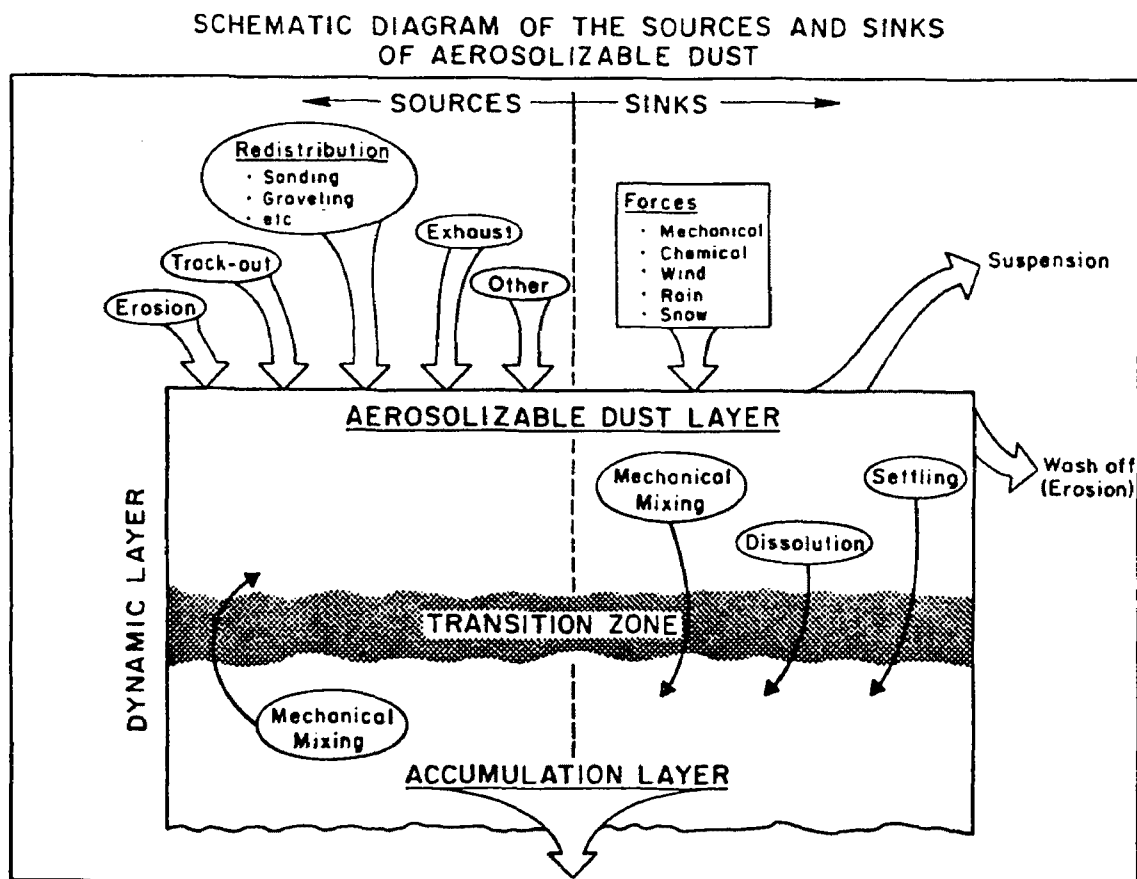


Figure 9. Schematic diagram of the sources and sinks of aerosolizable dust.

SILVER KING SCHOOL  
Percent Quarterly Lead  
(Geometric Means)

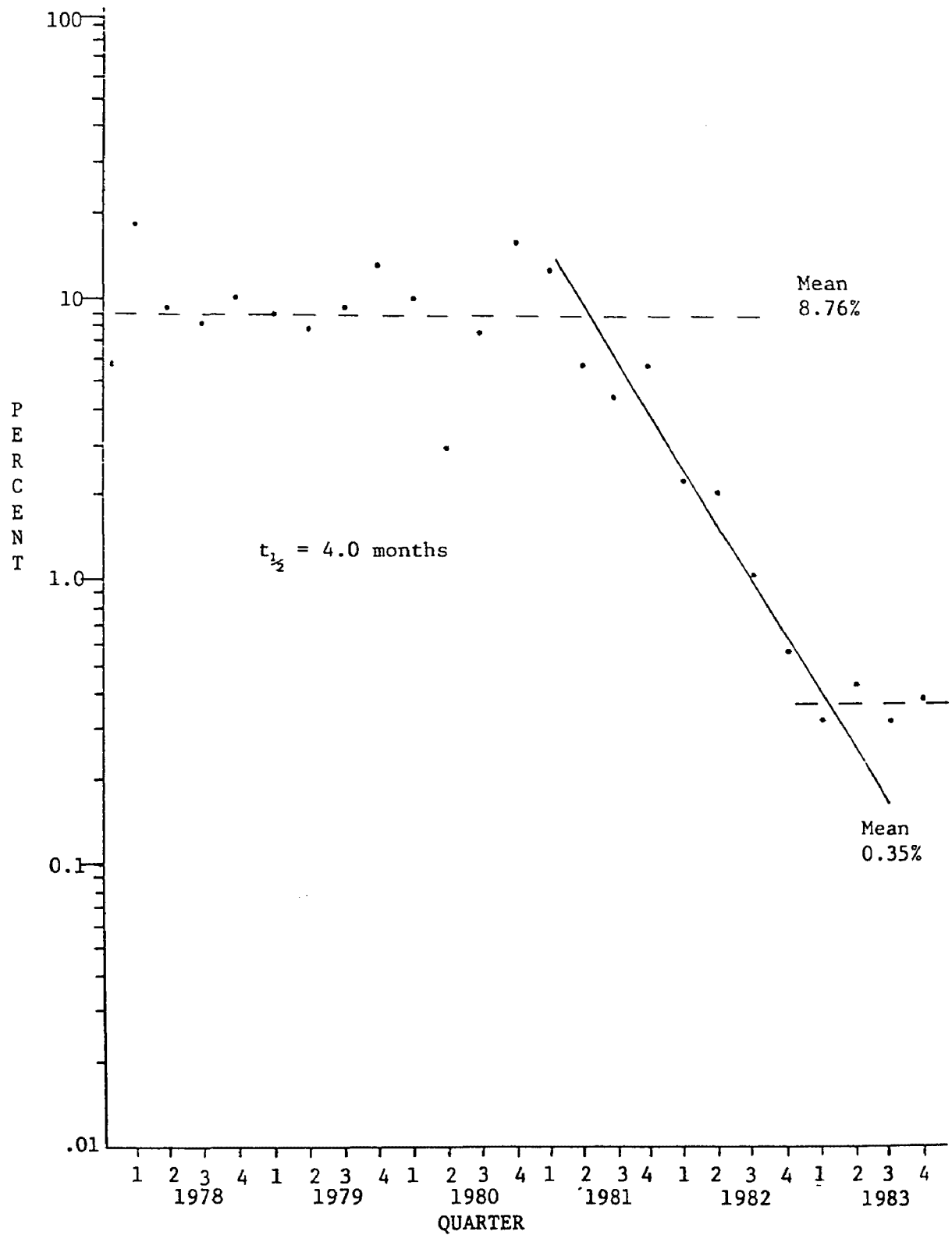


Figure 10. Percent quarterly lead levels at Silver King School Kellogg, Idaho

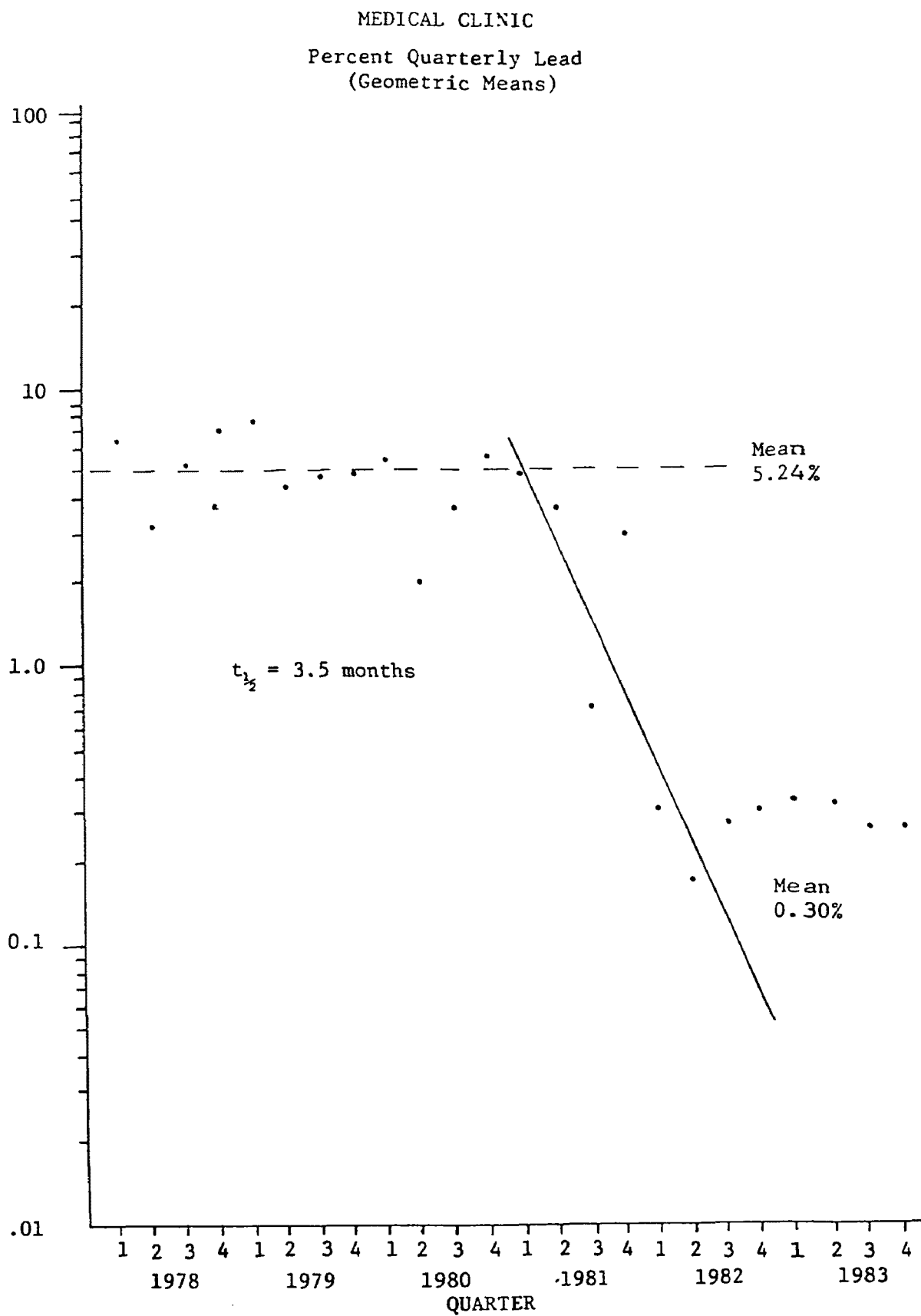


Figure 11. Percent quarterly lead levels at a doctor's clinic in Kellogg, Idaho.